

# Crud in PWR/VVER coolant

## Volume I – Sources, Transportation in Coolant, Fuel Deposition and Radiation Build-up

*Author*

Suat Odar  
Erlangen, Germany

*Reviewed by*

Peter Rudling  
ANT International, Mölnlycke, Sweden



A.N.T. INTERNATIONAL®

© November 2014

Advanced Nuclear Technology International  
Analysvägen 5, SE-435 33 Mölnlycke  
Sweden

[info@antinternational.com](mailto:info@antinternational.com)  
[www.antinternational.com](http://www.antinternational.com)

## **Disclaimer**

The information presented in this report has been compiled and analysed by Advanced Nuclear Technology International Europe AB (ANT International®) and its subcontractors. ANT International has exercised due diligence in this work, but does not warrant the accuracy or completeness of the information.

ANT International does not assume any responsibility for any consequences as a result of the use of the information for any party, except a warranty for reasonable technical skill, which is limited to the amount paid for this assignment by each Project programme member.

## Contents

<b>1</b>	<b>Introduction</b>	<b>1-1</b>
<b>2</b>	<b>Background information</b>	<b>2-1</b>
<b>3</b>	<b>Design and structural materials used in PWR, VVER and CANDU plants</b>	<b>3-1</b>
3.1	PWR plants	3-1
3.2	VVER plants	3-4
3.3	CANDU plants	3-8
<b>4</b>	<b>Sources of crud: Oxide layers on out-core surfaces</b>	<b>4-1</b>
4.1	Oxide film formation	4-1
4.2	Characteristics of oxide layers: Thickness, chemical composition and structure/morphology	4-5
4.2.1	Thickness of oxide layers	4-5
4.2.2	Chemical composition of the oxide layers	4-12
4.2.3	Structure/morphology of oxide layers	4-21
4.3	Influence of zinc chemistry	4-23
4.4	Influence of RCS structural materials on crud composition	4-25
4.5	Interaction with coolant	4-30
4.6	Metal release	4-36
4.7	Summary of section 4: Sources of crud; oxide layers on out-core surfaces	4-54
<b>5</b>	<b>Crud transportation in PWR/VVER coolant</b>	<b>5-1</b>
5.1	Colloids and their characteristics	5-1
5.1.1	General information	5-1
5.1.2	Surface charges and zeta potential	5-2
5.2	Plant monitoring data	5-5
5.2.1	Sampling techniques and limitations	5-5
5.2.2	PWR field data	5-14
5.2.3	VVER field data	5-47
5.3	Summary of section 5: Crud transportation in PWR/VVER coolant	5-50
<b>6</b>	<b>In-core crud deposition on fuel assemblies</b>	<b>6-1</b>
6.1	Mechanism of crud deposition and fuel crud characteristics	6-1
6.1.1	Crud deposition mechanism	6-1
6.1.2	Beneath fuel crud concentration mechanism	6-5
6.1.3	Fuel deposit composition and distribution	6-6
6.1.4	Influence of coolant chemistry on fuel deposits	6-14
6.2	Crud movement within the core	6-25
6.3	Consequence of fuel crud deposits on core performance	6-26
6.3.1	Historical PWR data	6-26
6.3.2	PWR experience	6-29
6.3.3	Axial offset anomaly (AOA)/Crud induced power shift (CIPS)	6-33
6.3.4	VVER experience	6-48
6.4	Summary of section 6: In-core crud deposition on fuel assemblies	6-58
<b>7</b>	<b>Core crud release and radiation field build-up</b>	<b>7-1</b>
7.1	Core crud release during power operation	7-1
7.2	Shutdown crud release	7-4
7.3	Radiation build-up	7-10
7.3.1	Mechanism	7-11
7.3.2	Influence of coolant chemistry on radiation field build-up	7-20
7.3.3	Occupational radiation exposure (ORE)	7-30
7.3.4	VVER information	7-32

7.4	Summary of section 7: Core crud release and radiation field build-up	7-41
8	CANDU experience	8-1
8.1	Summary of Section 8: CANDU experience	8-6
9	Conclusive summary	9-1
9.1	Oxide layers on the structural materials	9-1
9.2	Metal release and coolant crud transport	9-3
9.3	Fuel crud deposits	9-4
9.4	Core crud release and radiation build-up	9-8
9.5	CANDU plants	9-10
10	References	10-1
	Nomenclature	10-1
	Unit conversion	10-3

# 1 Introduction

According to anecdotes the acronym “CRUD” stays for the term “Chalk River Unidentified Deposits”, where first time in the PWR industrial history some deposits on the fuel assemblies in the research reactor of the Chalk River Laboratories of AECL<sup>5</sup> was observed. Since then this term is frequently used by PWR industry only for the corrosion products in the reactor coolant system. For the corrosion products in the feed-water or in the secondary side of the steam generators this term is not used.

The importance of an adequate coolant crud control (i.e. stable oxide layers to protect the structural material integrity, which produces the crud, and minimizing the core deposits) to achieve improved plant performance was already recognized at the beginning of PWR operations in 1960s. Accordingly, since then lot of investigations were performed and are still on going to understand the stability behaviour of oxide layers in the reactor system as well as the complex function of their release, transport and in-core deposition.

ANT International published a Special Topic Report (STR) entitled: “CRUD in PWR/VVER and BWR Primary Circuits” in the LCC2 programme in 2006, which summarized the information available till end of 2005. Since 2005, significant plant experience was gained especially with respect to fuel deposits. The purpose of this two-volume report is to provide in the Volume I (issued in LCC10 programme) up-dated insight into different types of phenomena, like solubility, transportation, deposition and release of crud that helps to better understand the crud behaviour under PWR/VVER operating conditions. Published CANDU<sup>6</sup> plant field information were also considered in this report. The published up-dated information is summarized and evaluated with emphasis to practical aspects of the PWR/VVER operation.

The content of the Volume I report is:

- **Background information** (Section 2) describing the importance of coolant crud control;
- **Design and structural materials used in PWR and VVER plants** (Section 3) summarises the design and structural material features of the PWR, VVER and CANDU plants;
- **Sources of crud:** Oxide layers on out-of-core surfaces (Section 4) that describes mechanism for the formation of oxide layers on the surface of Reactor Coolant System (RCS) structural materials, mechanism of their release to coolant; and the influence of structural materials on crud composition;
- **Crud transportation** in PWR/VVER coolant (Section 5) that describes which form crud is transported and how crud is monitored including the limitation of sampling techniques;
- **In-core crud deposition on fuel assemblies** (Section 6), which describes the deposition mechanism, influence of core environmental conditions and/or coolant chemistry on the composition and distribution of fuel deposits. In addition, the crud movement within the core and the consequence of fuel deposits on core performance are explained;
- **Core crud release and radiation field build-up** (Section 7), describing the mechanism how out-core radiation build-up takes place;

---

<sup>5</sup> Atomic Energy of Canada Limited (AECL) is a Canadian federal Crown corporation and Canada's largest nuclear science and technology laboratory. AECL developed the CANDU reactor technology starting in the 1950s.

<sup>6</sup> The CANDU (short for CANada Deuterium Uranium) reactor is a Canadian-invented, pressurized heavy water reactor. The acronym refers to its deuterium-oxide (heavy water) moderator and its use of (originally, natural) uranium fuel.

- **CANDU experience** (Section 8) summarizes the published information on crud behaviour in CANDU plants in comparison to PWR plants;
- **Conclusive summary** (Section 9), concludes finally the information given in the Volume I of this two-volume report.

Volume II of this report is scheduled for the upcoming LCC11 programme in 2015/16, which describes in detail the mitigation tools for adequate crud control.

The information given in this two-volume report:

- Can support the plant chemists to establish their coolant chemistry strategy to achieve the plant specific goals.
- Is valuable for fuel vendors and plant fuel engineers to understand the influence of coolant chemistry on fuel performance.

## 2 Background information

All structural materials used in nuclear power plants are, as bare metals (steels and/or alloys), are not stable in the reactor water at operating temperatures and dissolve by corrosion. They are protected by passive oxide layers formed by the corrosion attack of the coolant. The protective effect of these oxide layers is based on their low solubility in the coolant and a slow reaction rate of any chemical interaction between the oxide layers and the surrounding environment. So, on one hand the corrosion products are forming tenacious protective oxide films on the structural materials and thereby assure the integrity of the system. However, on the other hand, these oxide layers dissolve in the reactor coolant to some extent and are transported as corrosion products (called also crud) to the reactor core. There, they deposit on the fuel assemblies and are activated. The deposition of the crud on fuel assemblies and their re-release to coolant influences highly the core and plant performance with respect to material integrity and radiation fields. Based on more than 50 years of PWR/VVER industry experience an inadequate coolant crud control can result in serious plant problems not only in-core but also out-of-core areas. The main PWR performance problems caused and/or influenced by crud are:

- **Primary Water Stress Corrosion Cracking (PWSCC)** of nickel based alloys in in-core and/or out-core areas, which occurs by degradation of protective oxide layers under tensile stresses at high temperatures;
- **High out-core radiation fields** due to deposited activated crud that cause exposure of the plant staff and maintenance personnel to ionizing radiation;
- **Heavy fuel deposits**, leading to higher fuel cladding temperatures due to increased thermal resistance, which may cause enhanced fuel cladding corrosion, pressure (and reactivity) drop across the core, and Axial Offset Anomaly (AOA)<sup>7</sup> generation.

The importance of an adequate coolant crud control, i.e. producing stable oxide layers to protect the material integrity and minimizing the core deposits to achieve improved plant performance was already recognized at the beginning of PWR operations in 1960s. Accordingly, since then lot of effort was done by collecting the operational field experience as well as materials testing in the laboratory to assess and to understand the stability behaviour of oxide layers in the reactor system as well as the complex function of their release, transport and in-core deposition. Based on achieved experience coolant chemistry was modified continuously to address the needs of adequate crud control. However, the economical demands forced the PWR industry to increase the core duty using more enriched uranium and/or MOX fuel assemblies for longer fuel cycles. This core duty evolution is somehow in contradiction to the demands of coolant chemistry for adequate crud control and makes extremely difficult to achieve the coolant chemistry goals. Therefore, it is essential to understand the crud behaviour at different locations, with changing chemistry conditions (pH<sub>T</sub> and Redox Potential) around the non-isothermal Reactor Coolant System for tailoring the coolant chemistry program plant specific to achieve at least acceptable results of crud control.

The crud behaviour in the PWR Reactor Cooling System (RCS) can be described in multi-step processes as follows (see Figure 2-1):

- Generation of passive oxide layers on out-core surfaces;
- Release to reactor coolant from the oxide layers;

---

<sup>7</sup> The term “Axial Offset” (AO) is the difference in power between the top half of the core and the bottom half of the core divided by the total core power. (AOA) is a situation when there is an unexpected downward shift in the PWR reactor core axial power distribution occurs.

- Transport in soluble and insoluble colloidal form by coolant to core;
- In-core deposition on fuel assemblies, where activation takes place;
- In-core release from fuel assemblies;
- Transport in soluble, and insoluble colloidal form by coolant to out-core areas;
- Deposition on (or incorporation in) oxide layers of out-core surfaces, and radiation build-up.

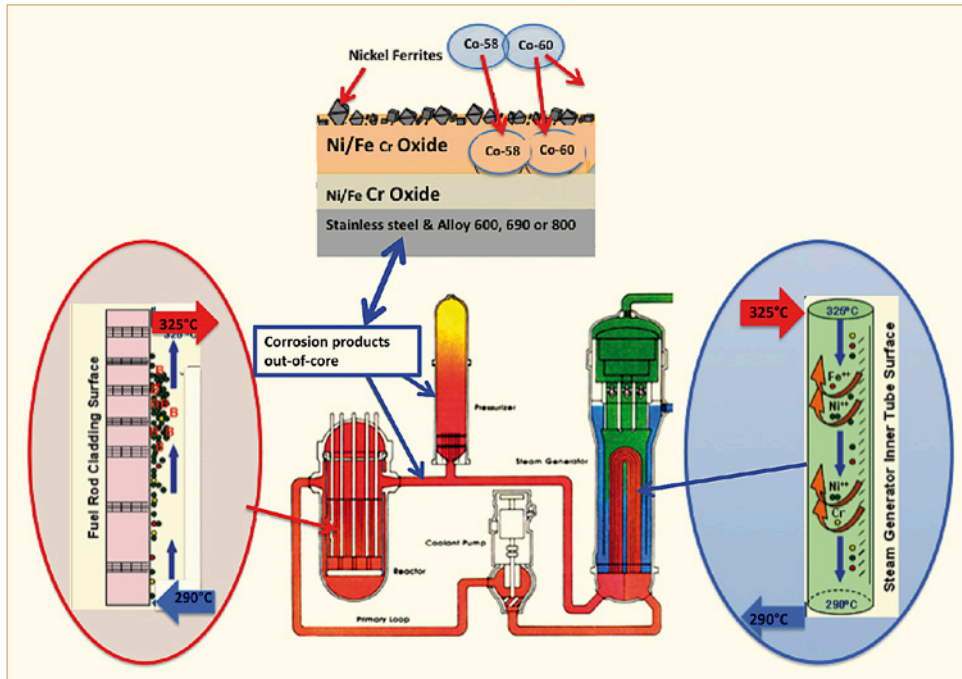


Figure 2-1: Schematic explanation of radiation build-up in PWR plants (figure modified by author using figures from different sources: [EPRI, 2006a], [Wood et al, 2008] and [Bengtsson, 2009].

A number of publications were performed through 1960s to 1990s describing the surveys and field experiences gained on these processes; especially on the out-core radioactivity build-up. These studies have shown that during steady state power operation the concentration of the corrosion products in the coolant are extremely low; i.e. iron in the lower ppb ( $\mu\text{g}/\text{kg}$ ) range whereas both nickel and cobalt are even in ppt ( $\text{ng}/\text{kg}$ ) range. The coolant concentrations vary widely from reactor to reactor with little correlation with the plant age. The concentration is also dependent on the  $\text{pH}_T$  and temperature of the coolant. Although evidence was also recognized that smaller ( $<5 \mu\text{g}/\text{kg}$ ) insoluble corrosion product particles are dominant ( $\sim 90\%$ ) early in reactor life [IAEA, 1992], the percentage of the larger particles increases with the plant age. In addition, these studies also indicated that in order to obtain an insight and understanding of coolant crud influence on the PWR plant performance it is necessary to understand the crud behaviour of both in soluble and in insoluble colloidal form.

In the time period between 1990s up to recent, where the PWR industry started to increase continuously the core duty due to economical reasons, severe AOA problems were experienced in PWR plants with nickel based SG tubing. Based on all these published information, these crud behaviour processes will be described in the following sections.

### 3 Design and structural materials used in PWR, VVER and CANDU plants

Structural materials used and the applied operational conditions such as temperature, redox potential and coolant chemistry are influencing the composition of the oxide layers build on the reactor coolant system surfaces. These oxide layers are the sources of the corrosion products that are circulating in the coolant and build deposits on the fuel assemblies, which impact the fuel and plant performance. In this section the design and structural materials used in PWR, VVER and CANDU plants are summarized in order to better understand the differences and similarities in crud behaviour observed in those three different plant designs that are discussed in subsequent sections.

#### 3.1 PWR plants

The reactor coolant system of PWR plants consists of a reactor pressure vessel, steam generators, pressurizer, main coolant pump and connecting loop piping as is shown schematically in Figure 3-1.

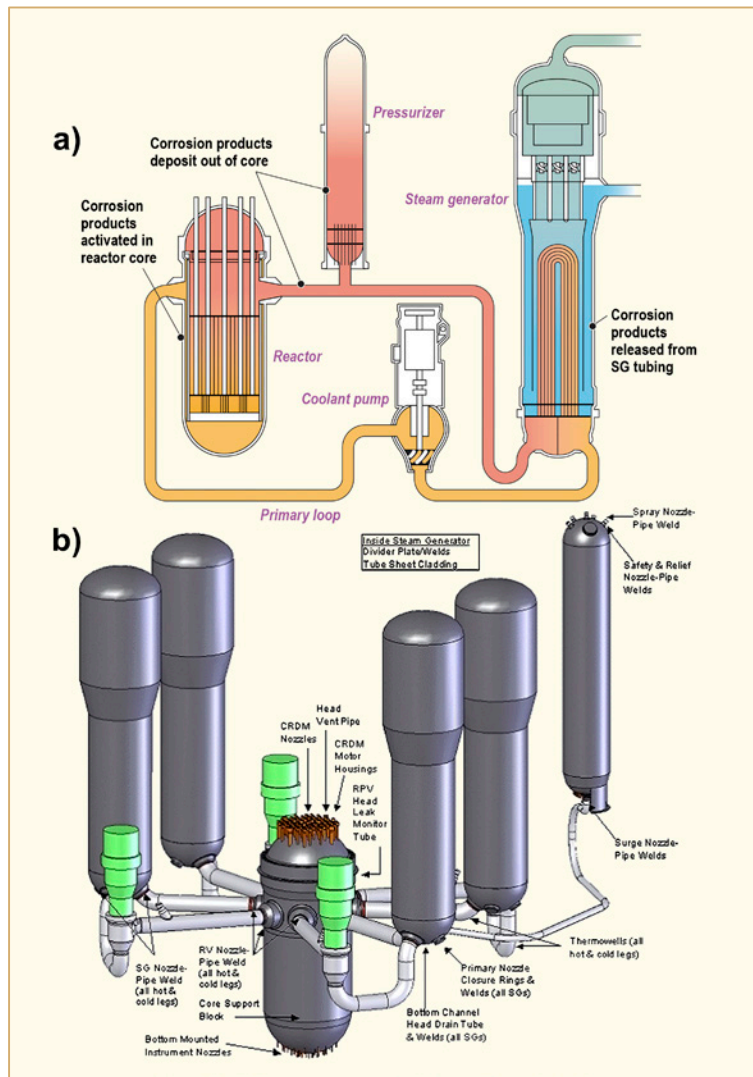


Figure 3-1: Schematic design of PWR reactor coolant system [Garbett, 2006].

All these big size components, except steam generator tubing, are built by carbon steels or low-alloyed steels that are clad by stainless steels on their surfaces in contact with the reactor coolant to provide excellent uniform corrosion resistance to the normal PWR water chemistry. The stainless steel cladding, usually 18-8 type is applied by weld overlay and is approximately 5 mm thick. The connected nuclear auxiliary systems like Chemical and Volume Control System (CVCS) and Residual Heat Removal system (RHR) are built with stainless steels. The compositions of stainless steels that are commonly used in PWR plants are given in Table 3-1.

Table 3-1: Composition of important alloys in contact with primary coolant, see Strasser in Section 3 in [Lundgren et al, 2005], courtesy by Westinghouse.

Stainless steels	Composition (%)										
	Ni	Cr	Fe	Mn max	C max	S max	Si max	P max	Mo	Nb	Ta max
304	8-11	18-20	bal	2.00	0.08	0.03	1.00	0.04			
304L	8-11	18-20	bal	2.00	0.03	0.03	1.00	0.04			
308	10-12	19-21	bal	2.00	0.08	0.03	1.00	0.04			
316	11-14	16-18	bal	2.00	0.08	0.03	1.00	0.03	2.0-3.0		
316L	11-14	16-18	bal	2.00	0.03	0.03	1.00	0.03			
321	17-19	9-12	bal	0.50	0.08	0.03	1.00	0.04		Ti=5×C min	
347	9-13	17-20	bal	2.00	0.08	0.03	1.00	0.03		10×C	
348	9-13	17-20	bal	2.00	0.08	0.03	1.00	0.04		10×C	0.10
410	0.5 max	17-20	bal	1.00	0.15	0.03	1.00	0.04			
17-4 PH	3-5	15-18	bal	1.00	0.07	0.03	1.00	0.04	Cu 3-5	Nb + Ta 0.15-0.45	

ANT International, 2011

For the steam generator tubes either nickel base alloys (Alloy 600 MA/TT, Alloy 690TT) or iron base Alloy 800 NG are used. Alloy 800 NG is used only in Siemens-KWU designed PWR steam generators. All other PWR plants designed by Westinghouse and its licensees (Framatome, Mitsubishi Heavy Industry) and also by Babcock & Wilcox (B&W) and Combustion Engineering have steam generator tubing with nickel base alloys. The detailed chemical composition of Alloy 600MA/TT (MA: Meal Annealed; TT: Thermal Treated), Alloy 690TT and Alloy 800NG (NG: Nuclear Grade) is shown in Table 3-2. The steam generator tubing has with about 70% the biggest surface area of the reactor coolant system surfaces that is in contact with the reactor coolant. Accordingly it has the biggest impact on the chemical composition of the oxide layers on the structural surfaces and in turn also on the composition and behaviour of the crud circulating in the reactor coolant and depositing on fuel assembly surfaces. This influence of steam generator material on crud characteristics and behaviour will be described later in Sections 4 to 7.

In addition to steam generator tubing, nickel base alloys (Alloy 600 and others) are also used at several other locations of reactor coolant system as penetrations and nuzzles in all PWR plants designed by Westinghouse and its licensees (Framatome, Mitsubishi Heavy Industry) and also by Babcock & Wilcox and Combustion Engineering. These locations are indicated in lower part of the Figure 3-1b. The composition of these nickel base alloys are given in Table 3-3. In Siemens designed PWR plants the use of these nickel base alloys as penetrations and nuzzles in reactor coolant system was avoided.

PWR plants are designed to use boric acid as chemical shim to control the core reactivity. The acidity of the boric acid is compensated by adding lithium hydroxide as alkalizing agent to control the reactor coolant pH<sub>T</sub> in alkaline region. For suppressing the coolant radiolysis and achieving the reducing conditions hydrogen gas is added into reactor coolant. The applied coolant chemistry has also influence on crud behaviour, which will be explained also in Sections 4 to 7.

Table 3-2: Chemical Composition of the Alloys 690 *TT*, 800 *NG* and 600, after [Stellwag et al, 1986].

Element	Alloy 690 <i>TT</i>	Alloy 800 <i>NG</i>	Alloy 600
C	0.01-0.04	0.03	0.01-0.05
Mn	0.50	0.4-1.0	1.00
P	0.025	0.020	0.025
S	0.015	0.015	0.015
Si	0.50	0.3-0.7	0.50
Cr	28-31	20-23	14-17
Ni	Bal.(>58)	32-35	Bal.(>72)
Mo	-	-	-
Fe	7-11	Bal.	6-10
Cu	0.50	0.75	0.50
Co	0.10	0.10	0.10
Al	0.50	0.15-0.45	0.50
Ti	0.50	0.60	0.50
Other	-	Ti/C ≥12 ; Ti/(C+N)≥8 N≥0.03	-

ANT International, 2014

Table 3-3: Compositions of nickel-base alloys commonly used in PWRs, after [Odar, 2014].

	Alloy X-750	Alloy 182	Alloy 82	Alloy X-718	Alloy 152	Alloy 52	Alloy 625
<b>Main components:</b>							
Nickel	72.5	>66	>73	52.3	>56.	>56	64.8
Chromium	15.5	13-17	18-22	18.5	28-31.5	28-31.5	22.5
Iron	6.4	≤10.0	≤3.00	22.5	8-12	8-12	2.5
<b>Minor components:</b>							
Titanium	2.5	≤1.0	≤0.75	0.89	≤0.50	≤1.0	
Aluminium	0.82			0.52		≤1.10	
Niobium plus Tantalum	0.97	1.0-2.5	2.0-3.0	5.12	1.2-2.2	≤0.10	
Molybdenum					≤0.50	≤0.05	8.7
Carbon	0.041	≤0.10	≤0.10	0.05	≤0.045	≤0.040	0.022
Manganese	0.75	5.0-9.5	2.5-3.5	0.05	≤5.0	≤1.0	0.75
Sulphur	0.001	≤0.015	≤0.015	≤0.015	≤0.008	≤0.008	
Phosphorus		≤0.030	≤0.030		≤0.020	≤0.020	
Silicon	0.3	≤1.0	≤0.50	0.1	≤0.65	≤0.50	
Copper		≤0.50	≤0.50		≤0.50	≤0.30	
Cobalt		≤0.12	≤0.10		≤0.020	≤0.020	

ANT International, 2014

## 3.2 VVER plants

VVER plants are a type of PWR that are in operation in Russia, Ukraine, Hungary, Slovakia, Czech Republic, Bulgaria, Armenia, Finland and China. Two major types are in operation or under construction, the 6-loop designs rated at 440 MWe (1375 MWth) and the later 4-loop designs rated at 1000 MWe (3000 MWth). Both designs are basically very similar with the main design difference of the number of steam generators: VVER 440 has six steam generators and VVER 1000 has four steam generators all in horizontal position. The design concept of these VVER plants is given schematically in Figure 3-2 the details are explained in the following.

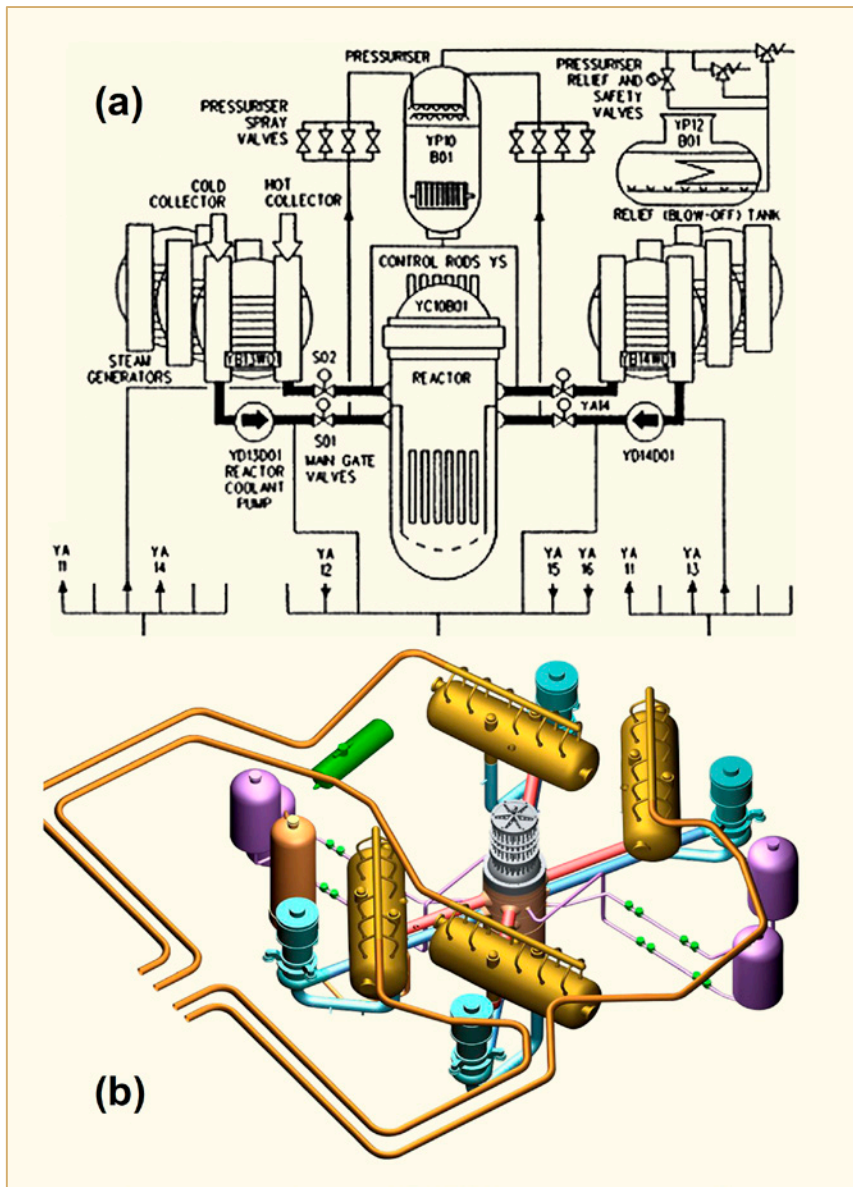


Figure 3-2: Schematic design of VVER 440 (a) and VVER 1000 (b) plants [IAEA, 2007].

Both VVER design plants are using boric acid as chemical shim to control core reactivity, similar to PWR plants. However, they use different concept for coolant chemistry: For alkalization of the boric acid potassium hydroxide is added, which is supported by lithium that is produced from  $^{10}\text{B}$  of boric acid by nuclear reaction in the core. In addition ammonia is added to produce hydrogen that is needed to suppress the water radiolysis and to establish reducing conditions.

### VVER-440 design:

There are two basic VVER-440 designs. These are the first generation VVER-440 plants, which includes the initial V-179 design, the V-230 design and the V-270 design with enhanced seismic features. The second generation VVER-440 is standard V-213 design with a full accident confinement system. The primary circuits of the VVER-440, V-179, V-230 and V-213 designs have a reactor pressure vessel (RPV) and six loops, each consisting of a hot leg, a horizontal steam generators (SG), and a cold leg in which is mounted a Main Circulating Pump (MCP). Two isolation gate valves are fitted to the hot and cold legs of each loop, one between the RPV and SG and one between the RPV and RCP. These enable individual loops to be drained for inspection and repair, whilst circulation is maintained in the other loops. There is no separate Residual Heat Removal (RHR) system and decay heat is removed via the SGs. A pressuriser (compensator tank) is connected to the cold leg of one of the loops and a spray line to the cold leg of the same loop. Typical operating conditions are  $T_{hot}$  297°C,  $T_{cold}$  267°C, 12.3 MPa. The compositions of the most important steels are given in Table 3-4 and cobalt impurity levels and surface areas are given in Table 3-5. All primary circuit surfaces in contact with the primary coolant are either made from stainless steel (main loop pipework, main coolant pumps, SG tubing, SG tube headers (collectors), gate valves and auxiliary systems pipework), from low alloy steel (RPV) or carbon steel (pressuriser, type-22K carbon steel) weld clad with stainless steel. Stainless steel components, pipework including SG tubing and the pressuriser clad are normally made from the Russian-type titanium stabilised stainless steel 08Cr18Ni10Ti, (08X18H10T equivalent to AISI (ANSI 321). The pipes of VVER-440 are made of 10Cr18Ni10Ti stainless steel with 500 mm inner diameter. The RPVs are made from low alloy steel (15Cr2MFA; Loviisa 12Cr2MFA), weld clad internally with two stainless steel layers.

Table 3-4: Composition of important alloys in contact with the primary coolant in VVER primary circuits, after [IAEA, 2007].

Alloy	Composition (percent by weight)								
	C	Si	Ni	Cr	Fe	Mn	Co	Others	Zr
07Cr25Ni13	≤0.09	≤1.2	11/14.5	22/26.5	bal.	0.8/2.0	≤0.05	-	-
08Cr18Ni10Ti (a)	≤0.08	≤0.8	9/11	17/19	bal.	≤1.5	≤0.05	Ti≥5C-0.6	-
08Cr19Ni10Mn2Nb	≤0.10	≤1	8.5/11	17.5/20.5	bal.	1.3/2.5	≤0.05	Nb=0.7/1.2	-
04Cr20Ni10Nb (b)	0.03	0.6	10	18	bal.	1.7	≤0.05	Nb=0.7	-
Zircaloy-4 (c)	≤0.027	≤0.012	≤0.007	0.07/0.13	0.18/0.24	≤0.005	0.002	Sn=1.2-1.7 Fe+Cr=0.28/0.37	bal.
ZIRLO	0.005/0.022	-	0.03-0.08	0.03/0.08	0.07/0.14	-	-	Sn=0.9-1.5 Nb=0.5/2	bal.
Zirc.1% niobium	≤0.05	≤0.05	≤0.025	-	≤0.07	≤0.002	≤0.007	Nb=0.8/1.2, O≤0.1	bal.
Zirc.2.5% niobium (b)	≤0.027	≤0.012	≤0.007	≤0.02	≤0.15	≤0.005	≤0.007	Nb=2.4/2.8, O=0.09/0.13	bal.

(a) Early VVER-440, V-230 units (excluding Bohunice 1 and 2) used 12Cr18Ni12Ti stainless steel; Loviisa used 08Cr18Ni12Ti for loop pipework.  
 (b) Russian data quote 04Cr20Ni10Mn2Nb (0.04%C, 20%Cr, 10%Ni, 2%Mn, 0.5%Nb).  
 (c) ASTM standard Zr-1%Nb is Russian type Zr-1%Nb.  
 (d) VVER-1000 primary circuit weld metal – 04Cr19Ni11Mo3.

ANT International, 2014

Table 3-5: Cobalt impurity levels in VVER plants, after [IAEA, 2007].

Alloy	Composition	Impurity level (percent by weight)		
		VVER-440		VVER-1000
		Specification	Loviisa (a)	
Stainless steel	Core internals	≤0.05	-	≤0.025
	Main coolant pipework	≤0.05	0-0.04	≤0.025
	RPV/SG clad	≤0.05	-	≤0.025
	SG tubing	≤0.05 (b)	0.03-0.06	≤0.025
	RCP bearing rings	≤0.05	0.0012-0.14	≤0.025
	Fuel assemblies/ Dummy elements	≤0.05	0-0.12	≤0.025
Zirconium 1% niobium	Fuel clad	-	<0.00003	-
Zirconium 2.5% niobium	Fuel assembly Outer sheath	-	-	-
(a) Actual values (b) Russian manufactured SG tubing in Paks 1 to 4: 0.04-0.06%Co. Russian manufactured SG tubing in Bohunice 1 and 2: 0.03-0.04%Co. Russian manufactured SG tubing in Dukovany: 0.05-0.07%Co Czech manufactured SG tubing in Bohunice 3 and 4; Dukovany 1 to 4: 0.15 to 0.02%Co. Dukovany 3 has three Czech and three Russian manufactured SGs. Dukovany 2 has five Czech and one Russian manufactured SGs. Dukovany 1 and 4 only have Czech manufactured SGs.				
ANT International, 2014				

### VVER-1000 design:

There are a number of VVER-1000 variants, the initial prototype V-187 design, the V-302 and V-338 designs and standard V-320 design. The new export V-392, V-428, V-466, V-412 variants have enhanced safety features, but are otherwise similar to the V320 design. All the VVER-1000 units have a full containment building [IAEA, 2007]. The primary circuits of all VVER-1000 designs have a RPV and four loops, each consisting of a hot leg, a horizontal SG, an intermediate leg, a main RCP and a cold leg. A pressuriser (compensator tank) is connected to the hot leg of one of the loops and the spray line to the cold leg and auxiliary sprays are connected to the charging line beyond the regenerative heat exchanger. VVER-1000 operating conditions are  $T_{hot}$  322°C,  $T_{cold}$  290°C, 15.7 MPa. As in most VVER-440, all primary circuit surfaces are either made from, or are clad in stainless steel. 08X18H10T stainless steel (08Cr18Ni10Ti, AISI321) is used for the core structures, main coolant pumps and SG tubing, whilst the main loop pipe work pressuriser and SG collectors are made from type 10GN2MFA carbon steel, clad internally with 08Cr18Ni10Ti stainless steel. The RPV is made from the low alloy steel 15Cr2MnFA, also clad with an inner layer of 07Cr25Ni13 stainless steel and two layers of the niobium stabilised stainless steel 04Cr20Ni10Nb (again similar to AISI 347). Small amounts of other grades of stainless steel and ferritic stainless steel are also present in the core internal structures, but no Stellite hard facing alloys are present in the primary or auxiliary circuits. The pipes of VVER-1000 are made of carbon steel with stainless steel cladding, 850 mm inner diameter.

Horizontal construction of the SG is technologically effective and safe in operation. However, if compared to the SG for VVER-440, the SGs of more powerful reactors (VVER-1000) have improved design that permits considerable intensification of heat exchange: smaller diameter tubes, and higher coolant velocity and steam generation temperature. This increased the heat-transfer coefficient by more than a factor of 1.7 and considerably increased thermal load at the same value of temperature drive. The dimensions of the heat exchanger increased only slightly, though the power increased considerably.

Standard VVER-1000 Russian fuel has zirconium-1% niobium clad and 08Cr18Ni10Ti spacer grids and end caps. There is no outer sheath in VVER-1000 units (except at Novovoronezh 5 where there is a perforated sheath allowing some cross flows). At Temelin, Westinghouse fuel has been ordered, which will have Zry-4 clad and spacer grids.

The influence of VVER materials on oxide layers on the system surfaces and on the behaviour of the crud circulating in the coolant and fuel deposits will be explained in Sections 4 to 7.

### 3.3 CANDU plants

In contrast to PWR and VVER plants, which have design similarities, CANDU plants have completely different design and structural material concept. First of all, CANDU plants are designed to operate with natural uranium fuel and they use heavy water as coolant and moderator. Due to use of extremely expensive heavy water the structural design limits the amount of heavy water by reducing the design volume of Heat Transfer system that corresponds to reactor coolant system of PWRs, to minimum as possible. Therefore, CANDU plants don't have reactor pressure vessel but their core is designed as pressure tubes that is called Calandria. The schematic design of the CANDU plants is shown in Figure 3-3 [Guoping Ma et al, 2012].

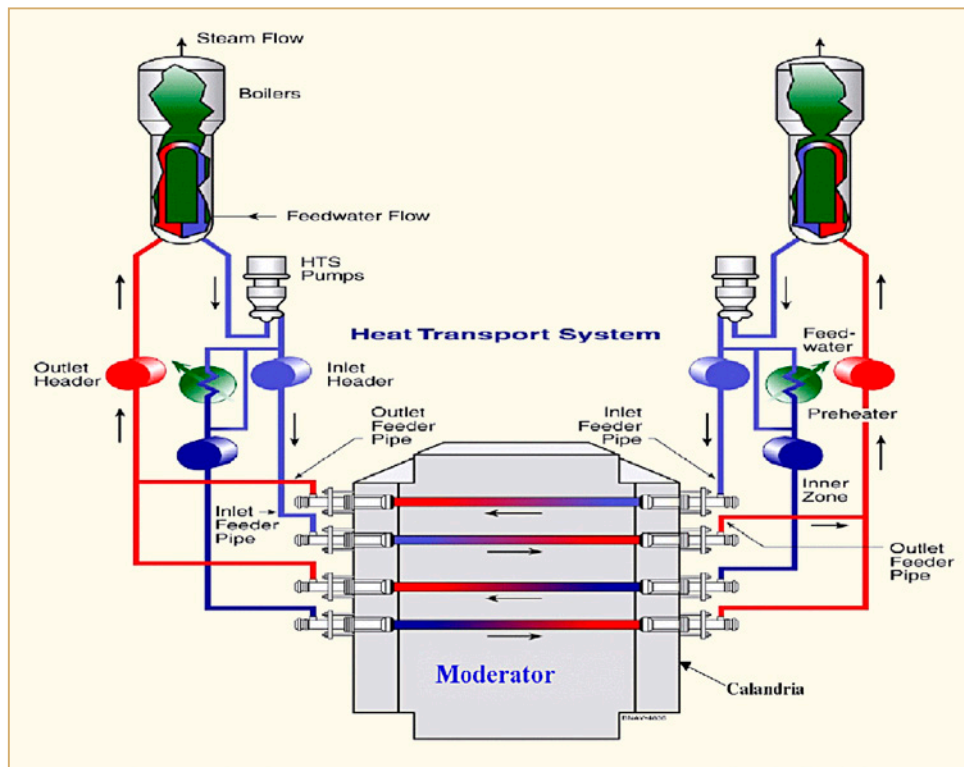


Figure 3-3. Schematic design of CANDU plants [Guoping Ma et al, 2012].

CANDU plants are designed to perform the refuelling continuously during the power operation. Accordingly they don't need to use boric acid as chemical shim to control excess core reactivity in contrast to PWR and VVER plants. The lack of boric acid in the reactor coolant enables to use carbon steels throughout the Heat Transfer System without any stainless steel cladding. The carbon steels are not used in the core and for the steam generator tubes. For Steam generator tubes and for the core pressure tubes following materials are used, respectively:

- Steam generator tubes: Monel 400 in Pickering A units (Monel 400: a nickel copper alloy with >63% Ni, 28-34% Cu and 1.0-2.5% Fe); Alloy 600 in Pickering B and Bruce units and Alloy 800 in Point Lepreau and Chantilly-2 units (composition of Alloy 600 and Alloy 800 is given in Figure 3-1).
- Pressure tubes: Zr-2.5 Nb and fuel cladding: Zircaloy

The influence of the design and materials on crud behaviour in CANDU plants will be explained separately in Section 8.

## 4 Sources of crud: Oxide layers on out-core surfaces

### 4.1 Oxide film formation

The major construction materials used in PWR reactor coolant system (RCS) materials are high alloyed CrNi-Steels, nickel based alloys, and in small quantities cobalt based alloys. In contrast to PWR plants, VVER plants are using only stainless steels as structural material including for their steam generator tubes. At ambient temperatures all these construction materials have very low corrosion rates because of the formation of the passive oxide layers that protect them. The thickness of these low temperature passive layers is in the range of several nanometres and their chemical composition is chromium rich (>30% Cr and usually free of nickel), either Cr<sub>2</sub>O<sub>3</sub> or a mixture of Cr<sub>2</sub>O<sub>3</sub> and hydrated chromium hydroxide [Kaesche, 1990], [Brüesch et al, 1984] and [Sato & Okamoto, 1981]. With increasing temperature above 150°C the general corrosion rate of these metals increase [Winkler & Lehmann, 1985] because the passive oxide layers become thicker and more porous but still protective. The composition and thickness of these protective layers depends on different factors, like the chemical composition of the base material, environmental conditions like the Electrochemical Corrosion Potential (ECP), pH and temperature of the medium to which they are exposed to. The thickness of these protective oxide layers is in the range of several hundred nanometres.

Due to the importance of corrosion product release for optimised fuel performance and control of radiation fields, the formation of passive oxide layers on structural materials under the condition of PWR environments have been of focused interest. Accordingly, there have been a number of engineering studies of metal-corrosion and metal- release in simulated PWR environments mainly in the time period of 1960s to 1990s. Some of the important ones as example are: [Jones, 1964], [Lister et al, 1987], [Bird et al, 1983], [Taylor & Armson, 1983], [Beslu et al, 1986], [McAlpine et al, 1984], [Polley & Pick, 1986] and [Lister, 1986]. Most of the investigations relate to nickel base materials, but stainless steel materials have also been included. The abundant use of carbon steel in US BWR designs and in CANDU plants has encouraged studies of carbon steels, [Zelenski, 1959] and [Vreeland et al, 1961].

According to these published studies, oxide layers built on structural materials under the PWR primary coolant operating conditions, i.e. reducing conditions at 300-330°C, have duplex structure as shown in one of the earliest schematic Figure 4-1 [Lister et al, 1987]. They have chromium-rich inner layer and an iron and nickel-rich outer layer. The existence of duplex oxide layers is a result of different diffusion rate of the cationic substituents of the alloy or steel through the chromium-rich inner protective oxide layer.

Growth of the oxide film proceeds mainly either at the metal/film or the film/solution interface, or both, although in principle the formation of a certain amount of oxide via internal oxidation reactions cannot be excluded. If the growth occurs solely via deposition of species originally present in the solution, no ionic transport through the solid phase of the film is required. In all other cases, the transport of ionic species through the film in the solid state is necessary to make film growth possible. If the diffusivity of the cation is much larger than that of the anion, the oxide growth occurs at oxide film/solution interface while the oxide growth occurs at oxide film/metal interface if the anion diffusivity is much larger (as is the case for Zr alloys). The diffusivity of the cation and anion depends on composition and structure of the oxide film. Transport of oxygen species from the film/coolant interface is needed for film growth at the inner interface (inner oxide layers). On the other hand, transport of cationic species from the metal/film interface contributes not only to the film growth but also to the dissolution of the film and subsequent formation of deposited outer oxide layers at the compact oxide/coolant interface. In order to enable the transport of ionic species in the oxide film, a certain minimum mobility of the species and a driving force is needed. Mobility is influenced mostly by the oxide film defect structure. The driving force in most cases is either a potential gradient resulting in the migration of species or a concentration gradient resulting in the diffusion of species. These driving forces can also exert a joint and simultaneous influence.

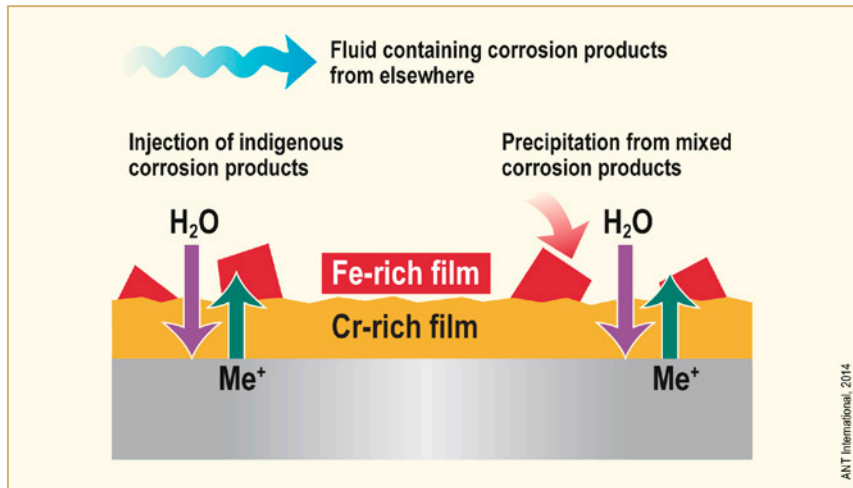


Figure 4-1: Structure of the protective oxide layers on stainless steel under PWR operating conditions, after [Lister et al, 1987].

The results of studies performed in the recent past has revealed that the chromium rich inner oxide layer actually consists of two layers (see Figure 4-2) [Combrade et al, 2005]: A few nm thick “Internal layer” also called “Barrier Layer<sup>8</sup>” with a chemical composition of  $\text{Cr}_2\text{O}_3$ ; “intermediate layer” or former “inner oxide layer” consists of chrome rich mixed spinel oxides (iron- and/or nickel-chromites and can be described by following formula:  $[\text{Ni}_{1-x}\text{Fe}_x][\text{Cr}_{2-y}\text{Fe}_y]\text{O}_4$ ). Accordingly, the oxide layers on the surface of structural materials consists of three layers if the “external layer” or former so-called “outer-oxide layer” is also considered, which has the chemical composition of spinel-type nickel ferrites. It is believed that the  $\text{Cr}_2\text{O}_3$  internal layer is actually the real protective passive layer. According to some researchers the protective character of the intermediate layer is not fully clear. However, due to the fact that chromium with its highest “Site Preferential Energy” for octahedral sites can stabilizes the spinel structure extremely good (explained in Section 4.2.3), a certain protective behaviour of the intermediate iron- and/or nickel-chromite spinel layers can be expected.

On bare metal surfaces, the oxidation exhibits several growth stages that seem to be typical of Ni base alloys: The  $\text{Cr}_2\text{O}_3$  internal layer is formed very rapidly on the bare surface and its thickness increases with the Cr content of the alloy. The oxide growth stops for a period of time probably due to temporary lack of chromium at the metal/oxide interface. Then after the oxide layer starts growing again with an oxidation controlled by anion transport through the inner oxide layer [Combrade et al, 2005]. The inner oxide layer grows at the metal/oxide interface as the water penetrates through the crystal defects such as pores and cracks in the oxide layer to the metal surface, where it reacts with the metal ions to build oxides. The formation of the crystal defects is attributed to increasing residual stresses in the growing oxide film that has bigger volume than base metal resulting in cracks [Asakura et al, 1989]. This inner oxide layer grows mainly by anion mass transport towards the oxide/metal interface although there is clearly iron and nickel cation transport in the reverse direction as illustrated schematically in Figure 4-3. The driving force for metal cation diffusion is the metal ion concentration difference between the metal surface and the coolant. However, the different chemical behaviour of the metal ions (iron, nickel and chromium) influences their diffusion behaviour across the inner oxide layers: In contrast to iron and nickel, chromium has smaller diffusion rate as trivalent cation ( $\text{Cr}^{3+}$ ) compared to divalent cations ( $\text{Fe}^{2+}$  and  $\text{Ni}^{2+}$ ) and builds extremely insoluble  $\text{Cr}_2\text{O}_3$  compound. Hence, chromium that is released from alloy surface builds immediately  $\text{Cr}_2\text{O}_3$  layers, whereas iron and nickel can diffuse further towards oxide/coolant interface. Subsequently chromium that is still uncompounded can build, because of its higher thermodynamically stability, iron- and/or nickel-chromites on  $\text{Cr}_2\text{O}_3$  barrier layer, before nickel-ferrites can be produced to build outer oxide layers. Therefore, the inner part of the protective oxide layer becomes chromium-rich, whereas the outer part is iron and nickel-rich and free of chromium.

---

<sup>8</sup> It is the “barrier layer” thickness that to a large extent determines the corrosion rate, since the “barrier layer” limits the transport of corrosion species. It is through the “barrier layer” that the diffusion of cations/anions takes place. A thicker “barrier layer” reduces the corrosion rate since the diffusion distance of the corrosion species increases.

## 5 Crud transportation in PWR/VVER coolant

As discussed Section 3, oxidized metallic elements are partly released mainly from the outer oxide layers of steam generator tube surfaces in the reactor coolant fluid. Nickel and iron are the main elements released, either in dissolved form such as  $\text{Ni}^{2+}$  and  $\text{Fe}^{2+}$  cations or in colloidal and/or particulate form (e.g.  $\text{NiFe}_2\text{O}_4$  species). The behaviour of these corrosion products in the reactor coolant during their transport will be explained in the following sub-sections.

### 5.1 Colloids and their characteristics

#### 5.1.1 General information

This subject is described in detail in Chapter 6 in [Hettiarachchi, 2013]. Here in this section only a summary is given regarding the colloid characteristics and their behaviour in PWR reactor coolant for better understanding the result of the plant corrosion product monitoring and radioactivity transport.

Colloids in nuclear power plants are the small size particles of molecular dimension that act as the dispersed phase suspended in flowing reactor coolant, which acts as the dispersed medium. They may be oxides, oxyhydroxides, mixed oxides and hydroxides. In PWR coolant colloids are formed continuously in various form and size as a result of the slow but gradual corrosion of structural steels and alloys that are exposed to high temperature coolant as described in see Section 4.1. The first step of colloid formation is the release of metal cations into the reactor coolant followed by hydrolysis of these cations forming various charged species such as sub-hydroxides or stable hydroxides. These species may undergo further oxidation to oxides and/or mixed oxides. Thus, reactor coolant usually has a multitude of charged species consisting of colloids and aggregates of colloids. These small size crud particles of molecular dimension have sizes from 1 to 1000 nm [Degueldre et al, 1996]. Species less than 1 nm in size are considered soluble while those that are bigger than 1000 nm are called suspended particles. Even though, per definition the species smaller than 1 nm are specified as soluble, they are actually still not soluble cations. Because the size of the corrosion product cations are in the range of 0.16 nm (see Table 5-1); and they don't exist alone as ions in the coolant. Due to their charge they interact with coolant building hydroxides, oxides, which may further agglomerate with other hydrated cations increasing their size. Thus, they still should be considered as colloids, even they cannot be monitored as colloids.

Table 5-1: Radius of divalent zinc, iron, nickel and cobalt ions, after [Lister, 2004].

Divalent cations	Ion radius [nm]
$\text{Fe}^{2+}$	0.087
$\text{Ni}^{2+}$	0.078
$\text{Co}^{2+}$	0.082
ANT International, 2014	

The size of the colloids depends on many factors such as the age of the species and their tendency to aggregate based on the pH value of the coolant, which will be explained later in connection with surface charges and zeta potential. The size distribution can be evaluated by sampling water through different filter mesh sizes using normal reactor coolant system sampling points (see Section 5.2).

Colloids also have very large surface area to mass ration and hence they don't precipitate easily, thus have certain stability within their stability pH range. This large surface area of colloids is partly responsible for their strong interaction with surface oxides and more important with radionuclides such as radio-cobalts in reactor coolant thus acting as a carrier in activity transport process.

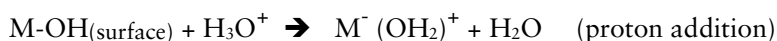
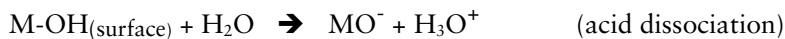
Colloids can be broadly separated into two categories, those that interact with water strongly (called hydrophilic) and those that don't have any tendency to interact with water (hydrophobic). However, in some cases there are colloids where one part is hydrophilic the other part is hydrophobic.

All type of colloids, particularly hydrophobic ones, can typically be subjected to two main types of forces: “van der Waals attraction” and “electrostatic repulsion” due to presence of their surface charges. The surface charge generation is due to dissociation of water during its interaction at colloid surface, or due to preferential adsorption of coolant ions by the colloid. The balance between these two forces keeps the colloid system in a stable condition depending on the pH value of the coolant (see next Section 5.1.2). The presence of Brownian motion or thermal energy also contributes to maintain colloid stability. Changing the coolant pH value that may result in flocculation of the colloid species can destabilize the colloid system. For example, the particle size change of the coolant corrosion products by coolant pH increase during the fuel cycle was observed by sampling investigations at some PWR plants (see Section 5.2.2). The mechanism of the pH influence on colloidal stability is described in Section 5.1.2.

Unlike the case of ionic species that are usually single valent or multi-valent, colloidal surfaces can sustain much higher surface charges all around its surface. Because of the presence of electrical double layers form around the colloidal particles (see Section 5.1.2), these surface charges impart unique electrochemical properties on to colloidal systems such as, electrophoresis, electro-osmosis, streaming potential, zeta potential and sedimentation potential [Hunter, 1988].

### 5.1.2 Surface charges and zeta potential

Colloids in coolant suspensions consist of oxides, hydroxides, mixed oxides and oxyhydroxides has hydroxyl groups on their surfaces formed by surface hydration, very similar to the process that was discussed for the surface oxide layers on structural material (Section 4.5). These hydroxyl groups are ampholytes and can dissociate according to the following reactions:



These reactions create either positive or negative surface charges depending on coolant pH values. The negative charge on the oxide layer originates from the acid dissociation of the surface hydroxyl group [Parks, 1965]. The positive surface charge forms from receiving of a proton by the neutral hydroxyl group [De Bruyn & Agar, 1962]. Whereas at lower pH values protons are added on hydroxyl groups (i.e. building positive surface charge), acid dissociation takes place at higher pH values (building negative surface charge). At pH values where none of these reactions dominates or takes place, the surface has no charges; therefore, it is neutral. This point of pH value is called “Point of Zero Charge” (PZC) as schematically shown in Figure 5-1.

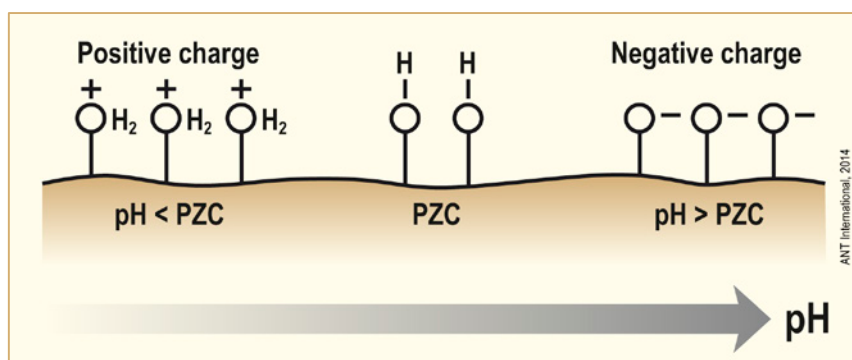


Figure 5-1: Influence of coolant pH value on surface charges, after [Hettiarachchi, 2013].

Soluble ions with opposite charge to surface charge that exist just in the proximity of the colloid oxide surface form a compact charged coolant layer to neutralize the colloid surface charge. This compact coolant charge layer is called Helmholtz layer (or Stern layer). However, the charge of this compact layer is not sufficient to neutralize the colloid surface charge because the ions in the coolant are continuously in movement. Therefore, some other coolant ions outside of the Helmholtz layer are contributing to the balance of the surface charges on the colloid surfaces. This mobile coolant charge layer is called “Diffuse Layer”, which consists of mobile positive and negative charged ions and remains in the proximity of the colloid surfaces. The result of this interaction between colloids and the coolant ingredients in the vicinity is illustrated in Figure 5-2. The boundary plane between Helmholtz and diffuse layers is called “Shear Plane” and the electrical potential difference between this Shear Plane and the bulk coolant is called Zeta ( $\zeta$ ) Potential. This Zeta potential and the colloid surface charges are responsible for the interaction of colloids with each other and/or for the adsorption of the colloids on the surface oxide layers on structural materials. With respect to electrostatic interaction there exists repulsive forces between the colloid surfaces with same charges and attraction between colloid surfaces with opposite charges.

As illustrated in Figure 5-1, the surface charges are affected by pH values of the coolant, and hence the sign and magnitude of the zeta potential is dependent from coolant pH values. Colloids and oxide surfaces with different chemical composition have also different PZC values. For example, the solid oxide layers on structural materials and the suspended colloidal particles that are formed in the coolant have different chemical composition and hence also different PZC values. The coolant pH dependence of the interaction behaviour of these two surfaces can be explained with the aid of Figure 5-3 as follows:

At coolant pH values  $<PZC1$  and at pH values  $>PZC2$  oxide layers on pipe surfaces and colloidal particles have the same surface positive and negative charges respectively. In this coolant pH range there exist repulsive forces between both surfaces; hence deposition of colloidal particles on pipe oxide surfaces is unlikely. In contrast to these conditions in the pH range between  $PZC1$  and  $PZC2$  whereas the oxide layers on pipe have positive charge, the particle surfaces have negative charges; resulting in electrostatically attraction between both surfaces. Therefore, deposition of particles on pipe oxide surfaces can be expected. In particular, this is important for coolant sampling lines with respect to representative crud sampling, where huge piping surface exposed to small sampling volume in the sampling line exists. In such hot sampling lines adsorption of colloids and/or corrosion product cations in the oxide layers on sampling line surfaces can take place and thus biased the sampling results.

In the following Section 5.2.1 failure that can take place during the coolant corrosion product monitoring explained and the criteria for representative sampling will be discussed.

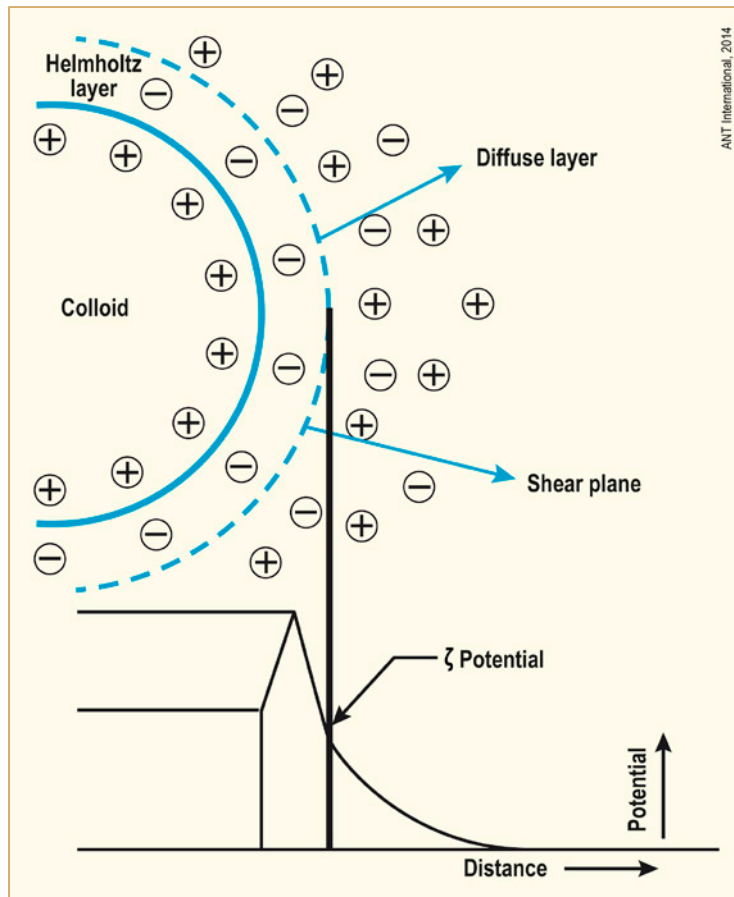


Figure 5-2: A schematic of electrical double layer generation around a colloidal particle and showing the origin of the zeta ( $\zeta$ ) potential, after [Hettiarachchi, 2013] and [Jayaweera et al, 1992].

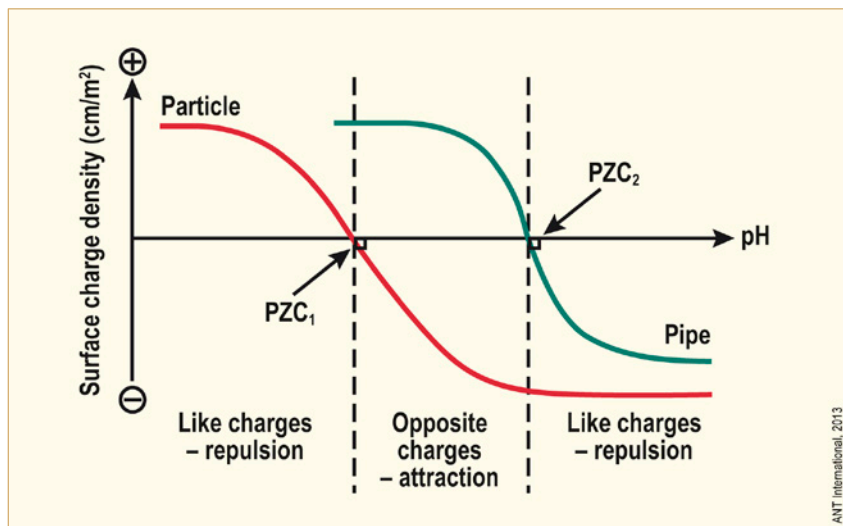


Figure 5-3: Charge titration curves for two surfaces (CRUD particles and oxide layers on pipe surfaces) having different Points of Zero Charges (PZC), after [Hettiarachchi, 2013].

## 6 In-core crud deposition on fuel assemblies

In the previous sections it was described that outer oxide layers on the structural materials stay in equilibrium with the reactor coolant that is saturated by corrosion products. The majority of the coolant corrosion products are in colloidal form with less than 0.2  $\mu\text{m}$  (200 nm) size in diameter. In the case of operational changes such as temperature or power changes or even makeup water injections and/or coolant chemistry changes like injection of chemicals this corrosion product saturation of the reactor coolant changes. This results in a sudden response from the outer oxide layers on the structural materials by either release of new corrosion products or their precipitation on reactor coolant system surfaces. Due to this equilibrium between the coolant and outer oxide layers on reactor systems the coolant corrosion product concentration is rather constant within a plant specific concentration range. The reactor core is a very efficient filter to collect the circulating coolant corrosion products. This results in a continuous release of corrosion products from the outer oxide layers to compensate the corrosion product removal by fuel assemblies due to explained equilibrium. In the following sections the mechanism of the corrosion product deposition on the fuel assemblies and the resulting consequences with respect to fuel performance and plant radiation build-up out of core areas are explained.

### 6.1 Mechanism of crud deposition and fuel crud characteristics

The reactor core is a very efficient filter when it comes to collecting the corrosion products transported in the coolant. The main parameter removing corrosion products from the coolant is the sub-cooled nucleate and nucleate boiling [Asakura et al, 1979], [Kawaguchi et al, 1983] and [Pan et al, 1985]. This is explained in the following section:

#### 6.1.1 Crud deposition mechanism

Since the earliest PWR operating experience in 1960s it is known that corrosion products in the coolant, so called crud, are depositing on the irradiated heat-transfer surfaces in the core area; i.e. on the fuel rod surfaces. The corrosion product deposition on the fuel rods is driven by boiling on the fuel surfaces and the crud mass is proportional to the degree of Sub-cooled Nucleate Boiling (SNB). Since SNB does not occur until the upper spans of the fuel assembly surfaces, crud is typically heavier in spans 5 and 6 as shown in Figure 6-1. The influence of boiling on fuel deposition can be explained as follows:

According to the Tentative Boiling model, as illustrated schematically in Figure 6-2a, once the steam bubbles grow (a), the colloidal Corrosion Product particles are trapped at the steam-water interface (b). These particles then move downwards to the heated fuel rod surface (c), where they deposit as the steam bubble with high speed grows and disappears (d). The deposition is similar for nucleate and sub-cooled boiling. However, it is faster for nucleate boiling. Once the particles come sufficiently close to each other they form agglomerates by the “van der Waals” forces. The crud deposits grow one layer after the other. As the deposit thickness increases, the boiling turns into so called “Wick Boiling”, where the water with soluble species of chemical additives and/or impurities if any, penetrates into oxide layers through capillary pores to the Steam Chimney (see Figure 6-2b). There, the water evaporates and leaves the chimney, while the soluble species concentrate.

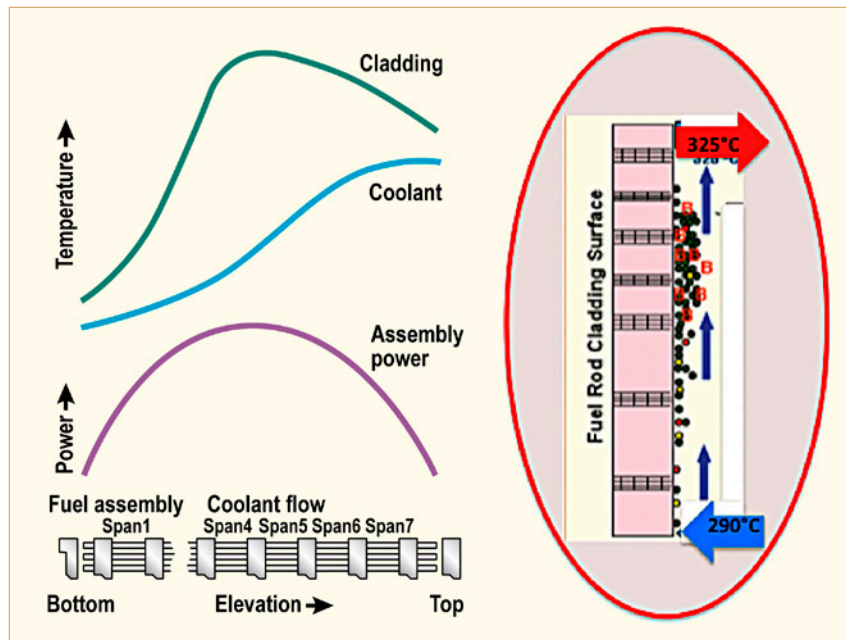


Figure 6-1: Simplified illustration of PWR fuel assembly temperature profile and corrosion product deposits [Odar, 2012a]. (Figure redrawn using the figures from [Bergmann et al, 1985] and [Bengtsson et al, 2008]).

The fuel rod deposits, not only on BWR but also on PWR fuel, contain a lot of such steam chimneys caused by Wick boiling (typically – 5000 per mm<sup>2</sup> [Macbeth, 1971]; looking visually like pores in the oxide surface. Fuel deposit sample gained from span 6 of Vogtle-2 PWR plant is shown as an example in Figure 6-3. These steam chimney pores enhance the heat transfer from the fuel rod into coolant and thus reduces drastically the thermal resistance of the crud layer. Due to these pores, the fuel deposits are porous with less density and high voidage. The estimated density of the PWR fuel deposits is in the range of 1.2 g/cm<sup>3</sup> [Hazelton, 1987], and the total voidage due to chimneys is approximately 10% [Macbeth, 1971].

The deleterious effect of deposits on fuel performance with respect to cladding corrosion and beneath deposit concentration mechanism depends on the characteristic of the crud:

In the case of thin deposits with many boiling chimneys, which provides excellent cooling of the fuel clad surfaces, the cladding surface temperatures do not exceed much above the coolant saturation temperature in the reactor core. In one reported case [Macbeth, 1971], the calculated temperature increase of the cladding was predicted to be 10°C instead of 100°C, which would be expected in case of thick and dense deposits. This is a most significant difference. The calculations have shown that wick boiling could actually support a heat transfer of 1–3 kW·cm<sup>-2</sup> (10–30 MW·m<sup>-2</sup>). This implies that wick boiling actually is more efficient than convective boiling, as expected on clean rods.

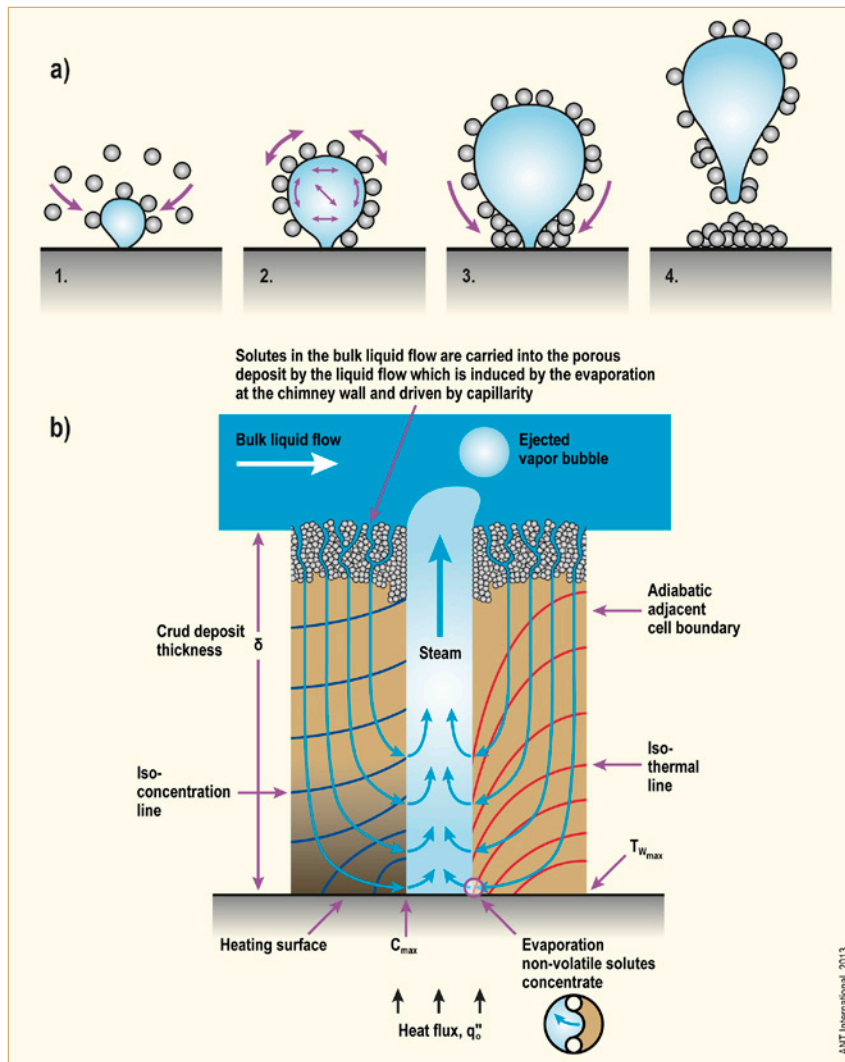


Figure 6-2: Fuel deposits: (A): Formation of deposits according to Tentative Boiling Model; (B): Principle of Wick boiling, after [Iwahori et al, 1979] and [Pan et al, 1985] respectively.

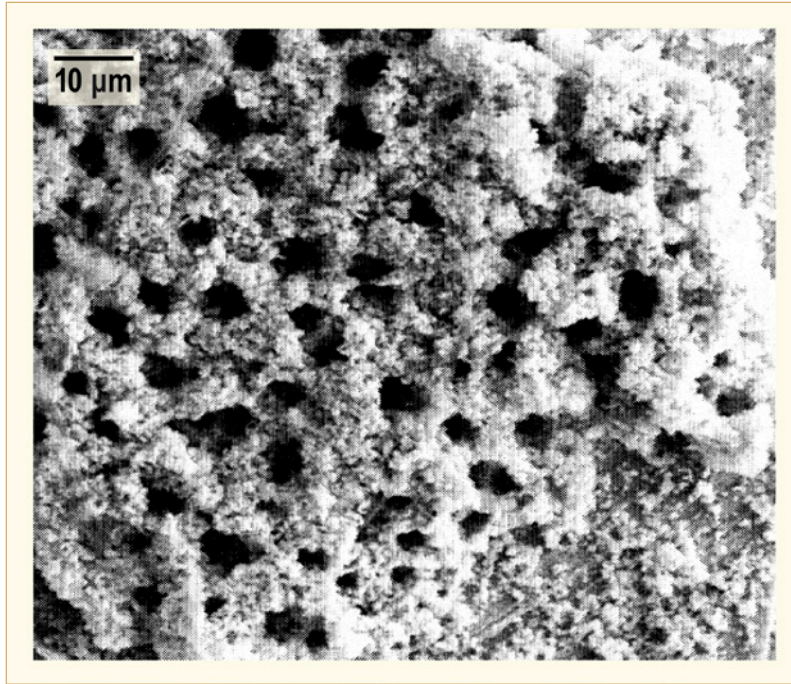


Figure 6-3: High magnification SEM of a CRUD flake obtained from Span 6B from Vogtle-2, Cycle 8 [EPRI, 2004a].

In contrast to reality of the fuel deposits with chimneys, if homogenous dense fuel deposits without chimneys are considered, the thermal residence of these deposits would be significantly resulting in deleterious consequences with respect to fuel corrosion performance. A Siemens (now AREVA) modelling of the End-of-Life (EOL) thickness of the  $ZrO_2$  film on Zircaloy-4 fuel rods with EOL burn-up of 55 MWd/kg U as a function of crud layer thickness is given in Figure 6-4. The results indicate that only few  $\mu\text{m}$  of such dense crud layer could be tolerated.

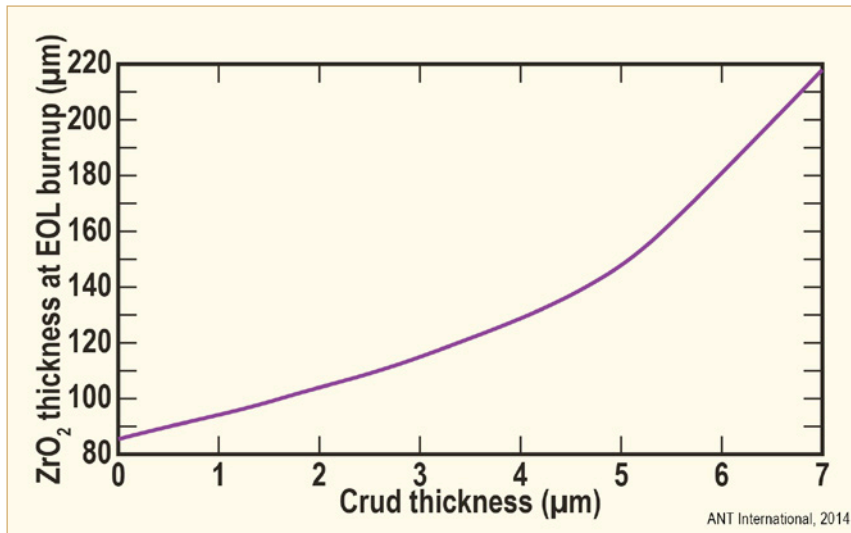


Figure 6-4: Siemens Modelling of  $ZrO_2$  oxide growth on fuel rods with EOL burn-up of 55 MWd/kg U as a function of crud thickness, after [Nieder et al, 1998].

## 7 Core crud release and radiation field build-up

### 7.1 Core crud release during power operation

Undisturbed steady state power operation conditions don't favour a release of corrosion product deposits from the fuel assembly surfaces. Quite in contrast, heat flux and sub-cooled nucleate boiling (SNB) favours the deposition mechanism. Hence, the crud deposits have tendency to remain on the fuel rod surfaces especially in the upper part 5<sup>th</sup> and 6<sup>th</sup> spacer grid area, where the highest heat flux and SNB is expected. However, in the case of some operational changes, such as power changes, injection of reactor make-up water that leads to dilution of the crud concentration in the coolant, which is actually saturated by corrosion products and also in the case of control rod movement, significant amount of crud deposits are released from the fuel surfaces for a short time. An example for the crud release from fuel rod surfaces by control rod movement for monthly "Control Rod Tests" reported from Ringhals Unit 2 is shown in Figure 7-1, [Bengtsson, 2002], and [Garbett et al, 2005]. The chemical composition of such fuel crud released by control rod movement at Ringhals Units 2 and 3 was reported by Studsvik to be consists of ZrO<sub>2</sub>, nickel ferrites and sometimes silicates, [Chen & Bengtsson, 2008]. In such crud release events the increase in coolant corrosion product concentration doesn't remain for a long time. Usually it flats down in a short time to the previous level of before disturbance (see Figure 7-1) by precipitation and/or adsorption on the oxide layer of the reactor coolant system surfaces including on the fuel assembly surfaces. This is due to the fact that the fuel crud deposits and the outer oxide layers on the structural material surfaces are in equilibrium with the reactor coolant, as confirmed by PWR field experience (see Section 5.2.2).

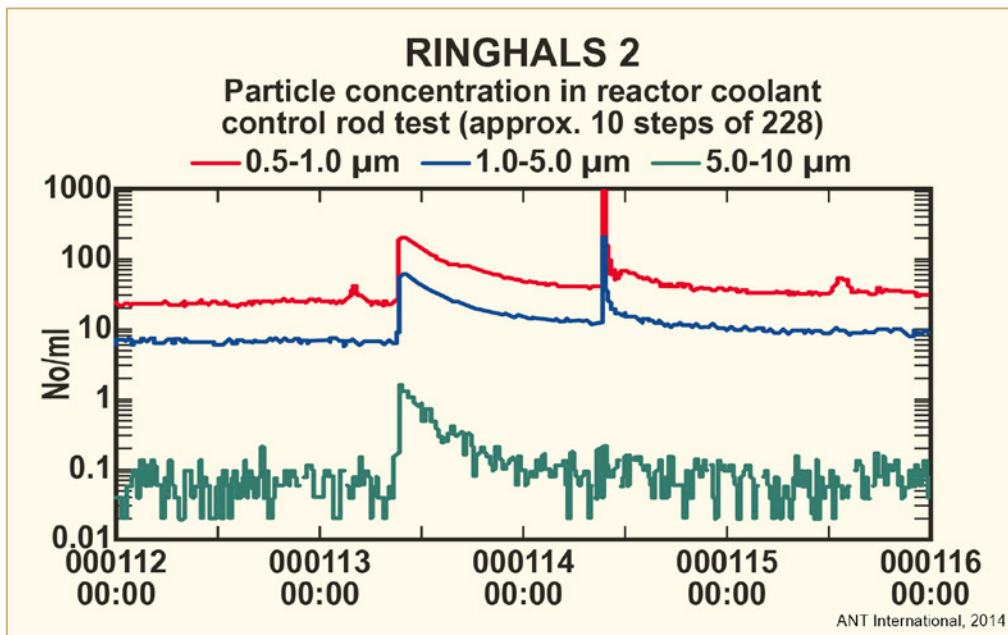


Figure 7-1: Particulate corrosion product release from the fuel rod surfaces by monthly control rod tests measured at Ringhals Unit 2, after [Bengtsson, 2002] and [Garbett et al, 2005].

Another possible mechanism for the release of fuel crud deposit during power operation is the local variation in sub-cooled nucleate boiling on fuel surfaces: For example after the boiling is stopped usually shear forces on the fuel surfaces can be increased, which results in mechanical release of fuel crud deposits. In such cases, particulate corrosion products are observed as indication for such release mechanism.

Coolant chemistry has an impact on fuel crud release also. For example increase in coolant  $pH_T$  results in iron solubility increase across the core with increasing temperature. Iron solubility of nickel ferrites is shown in Figure 7-2. This leads to decrease in fuel crud deposits by release due to increased solubility in the upper part of the fuel assemblies, where the boiling duty is higher. Applying such an adequate coolant  $pH_T$  decreases also the core residence time of the nickel ferrites.

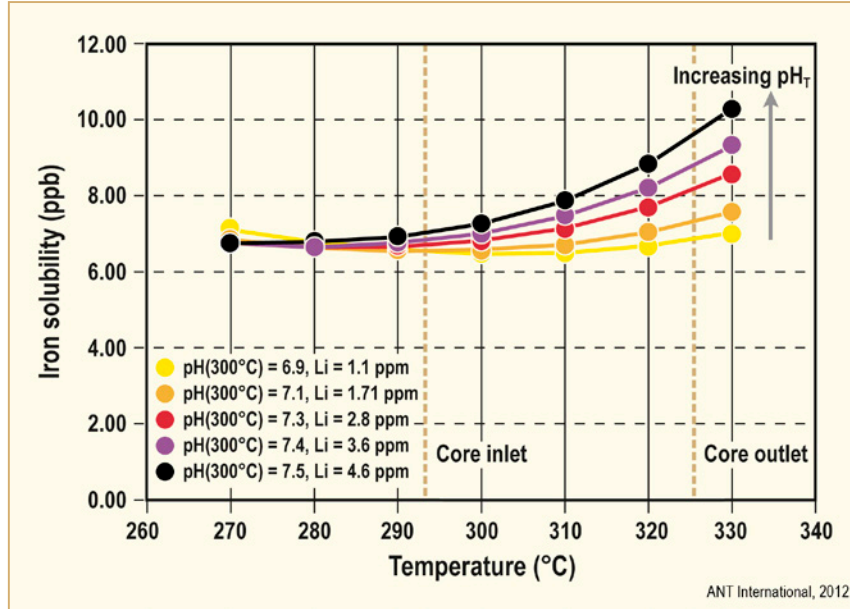


Figure 7-2: Iron solubility as a function of  $pH_T$  in the steam generator operating temperature range, after [Fruzzetti & Perkins, 2008].

Coolant chemistry modifications like decrease in dissolved hydrogen concentration and/or zinc injection can also increase the nickel release from the fuel crud deposits, as it was confirmed by fuel crud investigations performed by JAPC at their Tsuruga Unit 2 PWR plant in Japan, [Nagata et al, 2008]. They have found that before zinc injection the Ni/Fe ratio of significantly higher than 0.5 in the fuel crud deposits of the lower span area, which indicates an excess of nickel besides nickel ferrite that has Ni/Fe ratio of 0.5. After reducing the coolant hydrogen concentration there was a reduction of this Ni/Fe ratio in the lower span areas. Zinc injection later has decreased the Ni/Fe ratio even further down to that level of nickel ferrite (see Figure 7-3). This all confirms the increased nickel release from fuel crud deposits. The possible mechanism for these observations can be explained as follows:

Decrease in dissolved hydrogen concentration in the reactor coolant results in phase change of excess nickel from metallic to NiO in the fuel deposits (see Section 6.1.4.1), which is more soluble than metallic nickel under PWR operating conditions (see Figure 7-4). In the case of zinc injection into coolant this produces zinc chromite oxide layers by incorporation of zinc in the chromium rich inner oxide spinel layers, which is thermodynamically more stable oxide layers and accordingly protects the steam generator tubing material better against corrosion and metal release. The nickel source term reduction leads to decrease in coolant nickel concentration, which is probably compensated by release of excess nickel from the fuel crud deposits due to its equilibrium with reactor coolant.

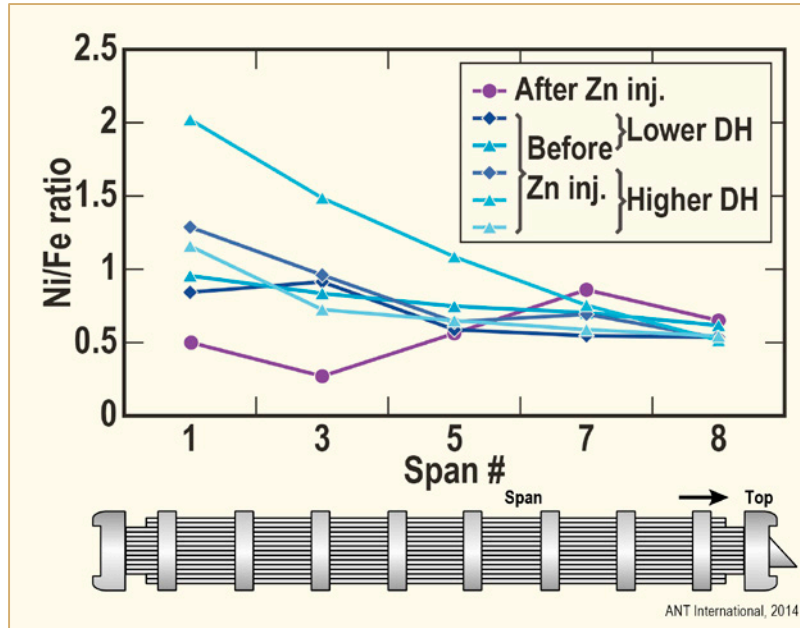


Figure 7-3: Measured Ni/Fe ratio in the fuel deposits before and after zinc addition at Tsuruga Unit 2 PWR plant, after [Nagata et al, 2008].

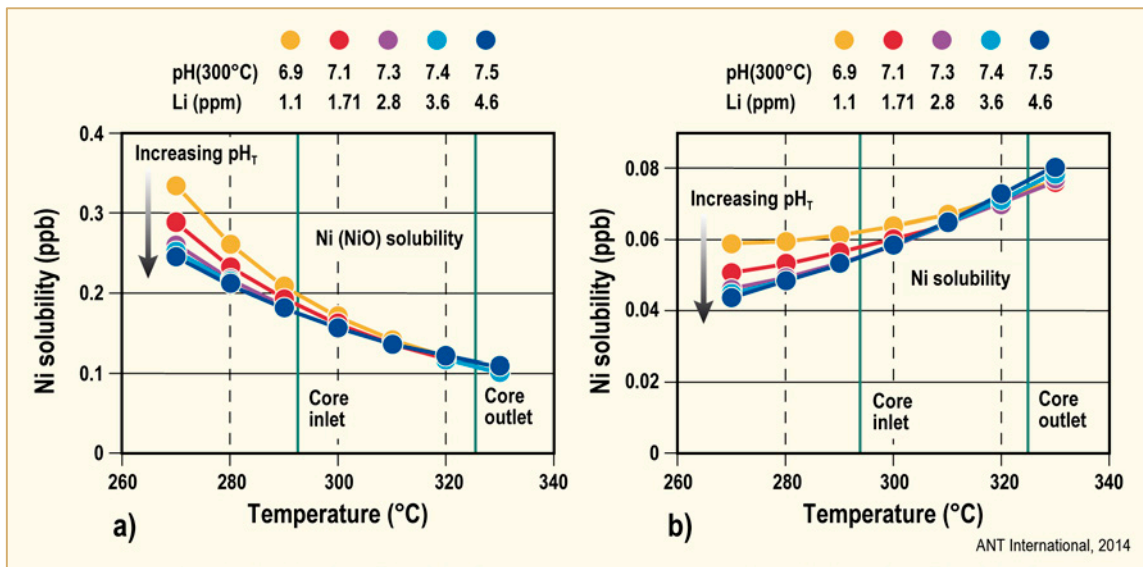


Figure 7-4: Variations in nickel solubility from core inlet to core outlet as a function of pH300 with boron concentration of 600 mg/kg and at (a): dissolved hydrogen concentration of 0 cc/kg (nickel as NiO); and at (b): dissolved hydrogen concentration of 35 cc/kg (nickel as metallic Ni) [Fruzzetti & Perkins, 2008].

It is obvious that all these possible mechanism for core crud release are plant specific. Accordingly the core residence time for the fuel crud deposits is also plant specific, which can vary from several hours and/or days up to several hundred days. For the estimation of the crud core residence time the specific activity of the corrosion products can be used. The calculated specific activities of several relevant corrosion product cations as a function of irradiation time are given in Figure 7-5, [Rochester, 2013]. For example, specific activity of <sup>58</sup>Co needs about 100 EFPD to come in equilibrium at a level slightly less than 1; whereas, in the case of <sup>60</sup>Co more than 10000 EFPD is needed and the level of the specific activity equilibrium is much higher.

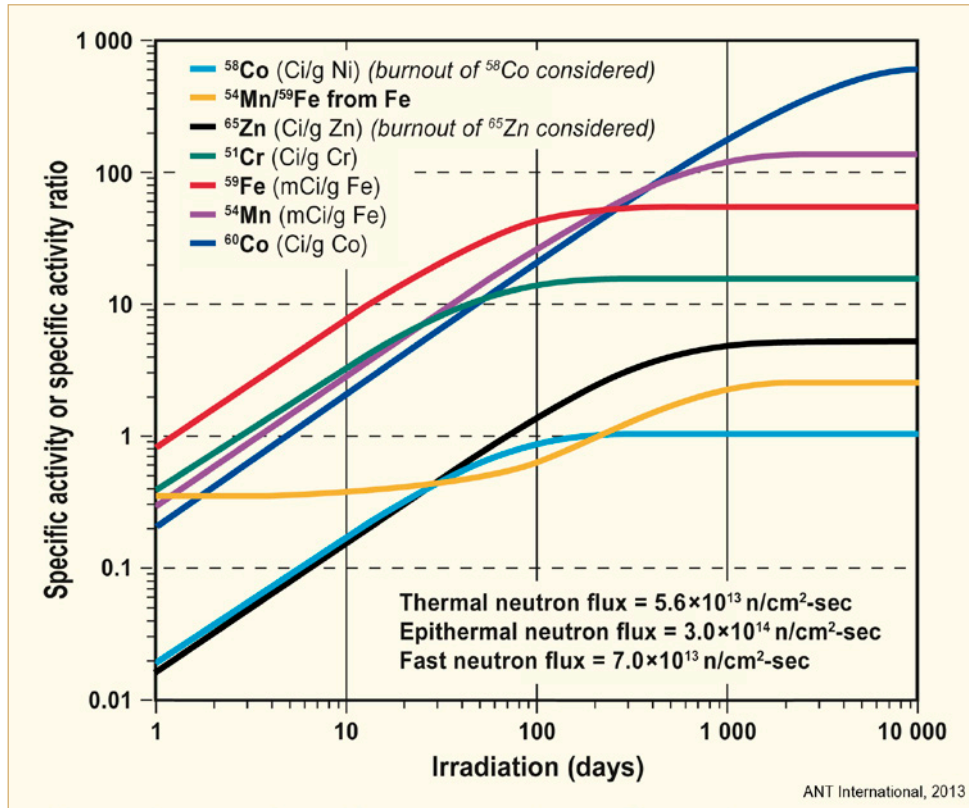


Figure 7-5: Calculated specific activity of major corrosion products (MBq/gram = Ci/gram × 3.7×104), after [Rochester, 2013].

## 7.2 Shutdown crud release

In contrast to steady state power operation, a cold shutdown causes significant changes of the physico-chemical conditions in total reactor coolant system especially in the core area. Four major steps are causing these changes of conditions:

- Power reduction
- Boration of the system
- Temperature decrease equivalent to a pH decrease
- Oxygenation (H<sub>2</sub>O<sub>2</sub> injection)

## 8 CANDU experience

CANDU Heavy-water Pressurized Water Reactor (HPWR) plants differ significantly in design, used structural materials and the water chemistry from the PWR plants. The CANDU plant design is shown schematically in Figure 8-1. This type of plants is designed with pressure tube reactors called Calandria where the fuel assemblies are located. The refuelling work is performed with fuelling machine on-line during the operation by pushing the fuel assemblies from one end to another of the pressure tubes. The Hot Feeder Pipes collect the coolant from each pressure tube at the outlet side and transfers via Outlet Header to hot channel head of the steam generators. From the outlet channel head of the steam generators the coolant is transferred again back to pressure tube core inlet via Inlet Header and Cold Feeder Pipes. CANDU plants have separate moderator circuit for reactivity control. Therefore they don't use boron in the circulating coolant for chemical shim. This makes the coolant chemistry and pH control ( $\text{pH}_{25}$ : 10.3 corresponding to  $\text{pH}_{300}$ : 7.4–7.8) very simple by adding lithium hydroxide at constant concentration (up to 2 mg/kg) during the power operation and during the plant shutdown operations. The structural materials used in CANDU plants are the following:

- Steam generator tubes: Monel 400 (in Pickering A units), Alloy 600 (in Pickering B and Bruce units) and Alloy 800 (in Point Lepreau and Chantilly-2 units)
- Pressure tubes: Zr-2.5 Nb and fuel cladding: Zircaloy
- Feeder pipes and all other reactor cooling system: Carbon steels

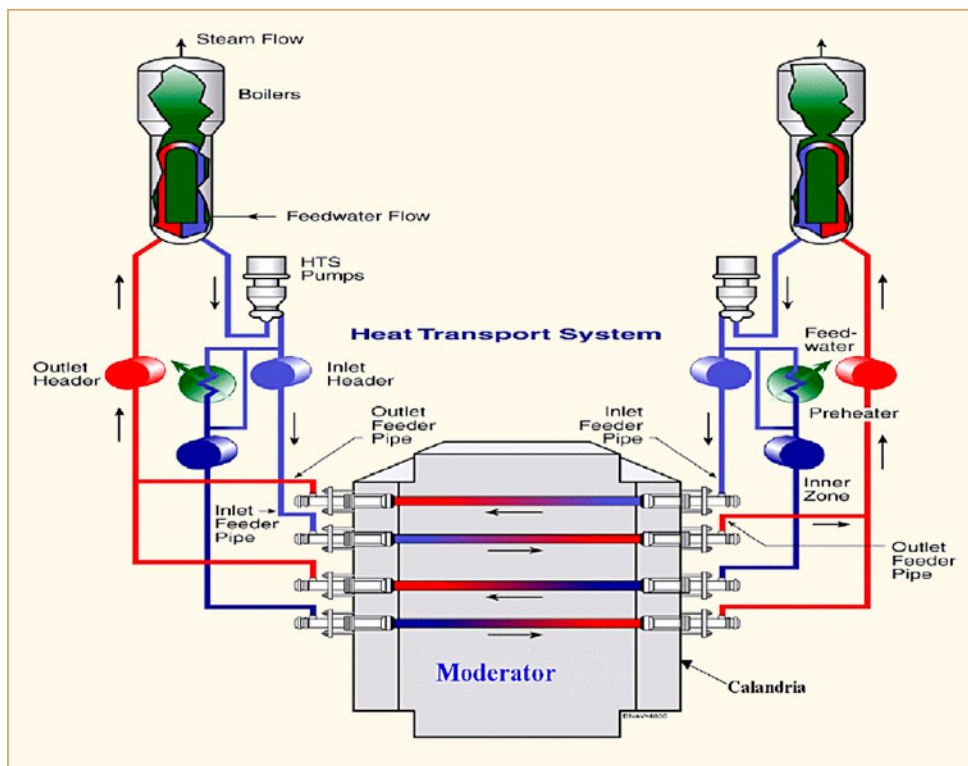


Figure 8-1: Schematic design of the CANDU reactors [Guoping Ma et al, 2012].

Regarding the oxide layers on the structural materials, the general observation in CANDU plants is the following:

After a several of years of operation, piping from about the location of the steam generator U-bend to the core inlet is covered with a two-layer oxide film consisting of a thick (100s of  $\mu\text{m}$ 's) layer of precipitated magnetite on top of a much thinner (1-10  $\mu\text{m}$ ) oxide layer that is formed by corrosion of the base metal, while on piping from the core outlet up to the steam generator U-bend the precipitated layer is thinner or absent (see Figure 8-2).

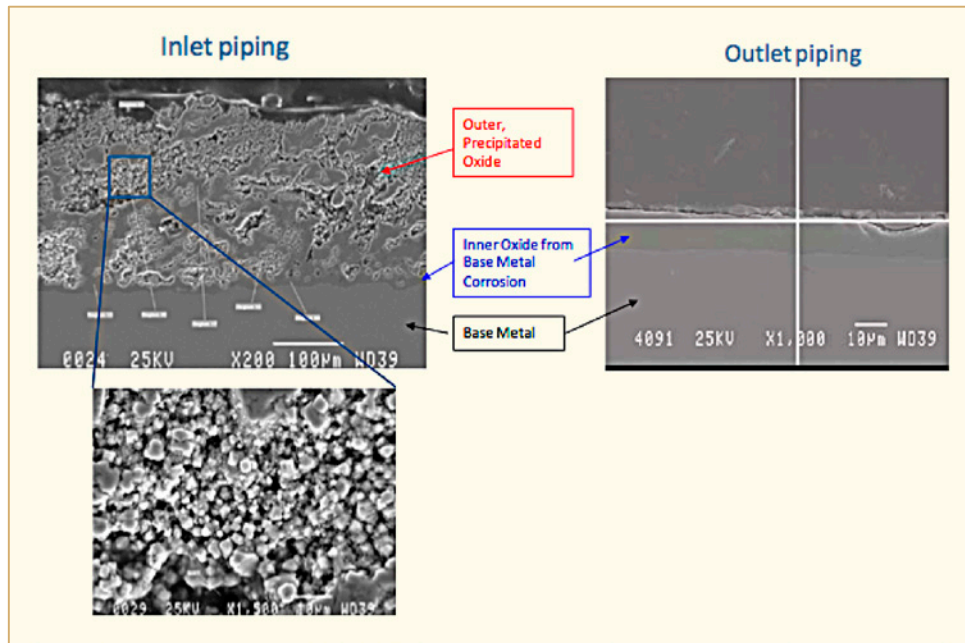


Figure 8-2: Cross-sections of typical oxide layers and deposits found on the core inlet and outlet piping of the CANDU HTS, [Guzonas & Qiu, 2010].

In general, three types of out-of-core heat transport system (HTS) surface with or without oxide layers can be defined:

- 1) “Bare” carbon steel surfaces (carbon steel outlet feeders and headers), which, because of Flow Accelerated Corrosion (FAC), are undergoing active corrosion and therefore, no oxide layers or deposits exist on these surfaces (indicated with red colour in Figure 8-1). Radionuclide deposition on these surfaces is negligible;
- 2) Other “bare” surfaces (e.g., stainless steel outlet end fittings, hot leg of steam generator tubes (Alloy 600, Alloy 800 or Monel 400), which have a corrosion layer similar in composition and structure to those found in PWR steam generator oxide layers (indicated again with red colour in Figure 8-1); and finally
- 3) Magnetite-covered surfaces Steam generator cold-leg tubes, inlet feeders, inlet end fittings surfaces that are covered with magnetite deposits (indicated with blue colour in Figure 8-1).

Model calculations indicate the solubility and precipitation behaviour of magnetite as responsible for this observation, [Guzonas & Qiu, 2010]. This is schematically illustrated in Figure 8-3. When the dissolved iron concentration is greater than the solubility limit, magnetite will precipitate on system surfaces. The predicted oxide loading is shown in Figure 8-3b, which is in good agreement with station observations, namely low deposition in the steam generator hot leg tubes, increasing deposition through the U-bend and into the steam generator cold leg tubes, with deposition continuing up to the core inlet.

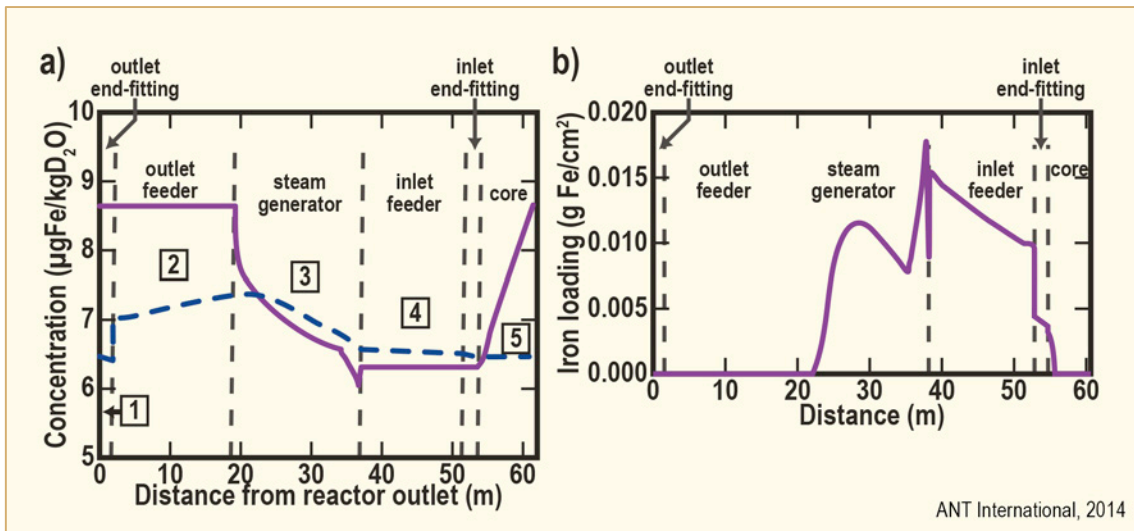


Figure 8-3 Model calculation result of (a): magnetite solubility limit (solid line) and iron concentration (dashed line) and (b): resulting oxide loading in CANDU 6 HTS, after [Guzonas & Qiu, 2010].

The magnetite solubility behaviour in different HTS regions indicated in Figure 8-3 a can be described as follows:

- 1) The coolant is under-saturated in dissolved iron as it leaves the core at 310°C.
- 2) The carbon steel outlet feeders undergo FAC, leading to an increase in the dissolved iron concentration in the 310°C coolant.
- 3) The coolant enters the steam generators at 310°C and leaves at 265°C. As the coolant temperature decreases in the steam generators, the coolant becomes super-saturated in dissolved iron. Magnetite deposition begins on the hot leg side and continues on to the cold leg side.
- 4) The coolant at 265°C that is super-saturated by dissolved iron passes through the inlet headers and feeders, depositing magnetite on all surfaces.
- 5) The super-saturated coolant at 265°C enters the core and is heated up to 310°C. There is some light deposition on the first metre in-core (pressure tube and fuel cladding) until the coolant temperature increases above the magnetite solubility limit.

The model calculated coolant iron concentrations are consistent with field measurements of corrosion product concentrations in the HTS coolant; which are during steady state power operation typically in the range 2-10  $\mu\text{g/kg}$ .

CANDU plant experience shows that iron is the main corrosion product circulating in the coolant of heat transport system (HTS), and that iron transport and magnetite deposition largely determine radionuclide (e.g.,  $^{60}\text{Co}$ ,  $^{95}\text{Zr}$ ) deposition and radiation field distribution around the HTS. In most CANDU plants,  $^{60}\text{Co}$  is the major contributor to CANDU HTS radiation fields. As in PWR plants,  $^{59}\text{Co}$  sources are either

- High surface area materials with trace concentrations of cobalt impurity, e.g., steam generator tubes with ppm levels of Co, or
- Low surface area materials with high concentrations of cobalt impurity, e.g., Stellite valve hard-facings or fuelling machine load balls, in which cobalt is a major constituent of the alloy.

The CANDU plant data indicate that the fuelling machine load balls are the largest  $^{59}\text{Co}$  source term in CANDU plants that dominates the radiation fields.

This oxide deposition pattern predicted above and observed in CANDU plants is very different from that reported for PWR plants. Figure 8-4 compares the activity build-up model reported by Bengtsson [Bengtsson et al, 2008] for PWRs, and the results of the CANDU activity build-up model [Guzonas & Qiu, 2010]. Whereas, in the case of PWR plants the steam generator tubing surfaces are the main contributors of corrosion products in the reactor coolant and they act in small extent also as “clean-up filters” for corrosion products. However, the fuel cladding surface are the most efficient ‘clean-up filters’ in PWR plants. In the case of CANDU HTS the steam generators are the most efficient ‘clean-up filters’ and the outlet feeders are the main contributors of corrosion products; the fuel assemblies in the core area are almost free of crud deposits.

This corrosion product behaviour in the CANDU HTS coolant is mainly due to the simpler coolant chemistry of the CANDU design; with a separate moderator system for reactivity control, which doesn't require boric acid in the coolant as chemical shim. The dissolved lithium concentration ( $\text{pH}_{25}$ ) of the HTS coolant is constant during steady state power operation and shutdown. This allows the HTS to operate at a  $\text{pH}_{25}$  high enough to ensure a positive solubility coefficient of temperature, which keeps the core free of deposits. While there is a small amount of deposition on the inlet fuel bundles, on-line refuelling eventually shifts the inlet bundles further into the core, where the deposits dissolve at the higher temperatures. In addition, magnetite deposition in the steam generators enables them to act as ‘full-flow’ purification ion exchangers, removing a significant fraction of both activated species (e.g.,  $^{60}\text{Co}$ ) and the inactive parent (e.g.,  $^{59}\text{Co}$ ). By removing nickel it also minimizes the deposition of nickel phases in the core and the production of  $^{58}\text{Co}$ .

The use of carbon steel as the inlet and outlet feeder material in the HTS of CANDU reactors results in magnetite deposition being the key factor determining radiation fields around the CANDU HTS, largely determining the spatial and temporal distributions of radionuclides on out-of-core surfaces. This is responsible for the observed continuous increase in radiation fields on steam generators and at the reactor face in CANDU plants. However, unlike PWRs, most of the magnetite deposits in the steam generators, allowing them to act as a “full-flow” purification system, removing most circulating radionuclides and their inactive parents from the HTS coolant.

However, this magnetite deposition on the primary side steam generator tubes caused also significant operational problems in several CANDU plants with respect to flow restrictions, ECT inspection difficulties. Therefore, in 1990's several CANDU plants were mechanically cleaned by Vacuum-Blasting techniques to remove these tube deposits (will be explained in Volume II of this report in the upcoming LCC11 program in 2015/16).

## 9 Conclusive summary

In the following sub-sections the information given in this report is conclusively summarized:

### 9.1 Oxide layers on the structural materials

- Under PWR operational conditions oxide layers build-up on the structural materials (stainless steels, nickel- and/or iron-based alloys) that protects the materials against corrosion. These oxide layers are consisting of duplex oxide layers, an inner oxide layer and overlying outer oxide layer. Actually the inner oxide layer consists of two sub-layers: “Internal” or “barrier” layer with chemical composition of  $\text{Cr}_2\text{O}_3$ ; and a chromium rich “intermediate” layer of mixed spinel oxides so called chromites. The “external layer” or former so-called “outer-oxide layer” has the chemical composition of spinel-type nickel ferrites and this layer is on stainless steels almost chromium free (<5% Cr) and on nickel-based alloys completely chromium free.
- The  $\text{Cr}_2\text{O}_3$  “internal” or “barrier” layer, which is built on the steels and/or alloys surfaces having  $\geq 10\%$  chromium has extremely thin thickness of few nm. The  $\text{Cr}_2\text{O}_3$  internal layer is formed very rapidly on the bare surface and its thickness increases with the Cr content of the alloy. It is believed that this  $\text{Cr}_2\text{O}_3$  internal layer is actually the real protective passive layer.
- The inner oxide layer (or intermediate layer) grows at the metal/oxide interface as the water penetrates through the crystal defects such as pores and cracks in the oxide layer to the metal surface, where it reacts with the metal ions to build oxides. It grows mainly by anion mass transport towards the oxide/metal interface although there is clearly iron and nickel cation transport in the reverse direction. The driving force for this metal cation diffusion is the metal ion concentration difference between the metal surface and the coolant. However, the different chemical behaviour of the metal ions (iron, nickel and chromium) influences their diffusion behaviour across the inner oxide layers: In contrast to iron and nickel, chromium has smaller diffusion rate as trivalent cation ( $\text{Cr}^{3+}$ ) compared to divalent cations ( $\text{Fe}^{2+}$  and  $\text{Ni}^{2+}$ ) and builds extremely insoluble  $\text{Cr}_2\text{O}_3$  compound. Hence, chromium that is released from alloy surface builds immediately  $\text{Cr}_2\text{O}_3$  layers, whereas iron and nickel can diffuse further towards oxide/coolant interface. Subsequently still unbound chromium can build, because of its higher thermodynamically stability, iron- and/or nickel-chromites on  $\text{Cr}_2\text{O}_3$  barrier layer. Therefore, the inner part of the protective oxide layer becomes chromium-rich, whereas the outer part is iron and nickel-rich and free of chromium. Overall thickness of the inner oxide layer varies with the surface conditions of the steels and/or alloys; and can be up to several nano-meters. Such different surface conditions are “as received”, electro-polished and mechanically polished.

- The **outer oxide layer** is a result of the interaction between the reactor coolant and the oxide layers; like solubility and precipitation of the corrosion products. The thickness of the outer oxide layer depends on the chemical conditions of the coolant such as redox potential and coolant nickel and iron concentrations; and also on the cation permeability behaviour of the inner oxide layers. It forms only in coolant saturated by corrosion products (nickel and iron) due to high solubility of the iron and nickel in spinels under reduced alkaline PWR coolant conditions. In iron-saturated coolant, large crystals of iron/nickel spinel oxide usually exist in this outer oxide layers that are produced by precipitation of corrosion products from the saturated coolant. Usually these outer oxide layers are thicker than the inner oxide layers. However, in the case of existing dense inner oxide layers (e.g. with zinc addition from the beginning on) these outer oxide layers are much thinner than the inner oxide layers as confirmed at the field. The chemical composition of these outer-oxide layers consists of a mixture of iron and nickel spinel oxides. The nickel content of this oxide layers depends on the steam generator tubing material that is used. In the case of VVER plants with stainless steel steam generator tubing, the nickel content of the outer oxide layers is very low; it can be described as magnetite that contains some nickel. If iron base Alloy 800 is used the outer oxide layers consist of nickel ferrites without excess nickel. In the case of nickel base steam generator tubing materials like Alloy 600 and Alloy 690, the nickel content is very high with Fe/Ni ratio  $\gg 0.5$  than that of nickel ferrites. In this case excess nickel exists as metallic nickel in addition to nickel ferrites in the outer-oxide layers. The outer-oxide layers have no protective behaviour for the structural materials. They are in equilibrium with the reactor coolant saturated by corrosion products and depending on the crud concentration of the coolant, which may change due to operational events, either they release corrosion products to coolant or corrosion products precipitate on the outer oxide layers. Accordingly they contribute highly to fuel deposits and in turn to out-of-core radiation build-up.
- The outer oxide layer has direct contact with the reactor coolant and in contrast to inner oxide layer, serves almost alone as crud source for the fuel deposits. The chemical composition of the fuel deposits that have insignificant amount of chromium indicates that inner oxide layers do not contribute significantly to crud transportation to core area
- The outer oxide layer is clearly influenced by coolant environment and its outer most layer is covered with hydroxyl groups by coolant hydration. The hydroxyl groups form by dissociation of the adsorbed  $H_2O$  molecules and chemisorption of the dissociated protons ( $H^+$  ions) on oxygen atoms in the neighbourhood. These surface hydroxyl groups are ampholytes being able to acid dissociation and/or to proton receiving thus creating negative and/or positive surface charges depending on coolant pH values. At pH values where the surface has no charges the point of pH value is called “Point of Zero Charge” (PZC).
- This oxide surface charges and the resulting Zeta potential are responsible for the adsorption of the charged coolant ingredients (corrosion products as soluble cations and/or as colloids) on the outer oxide layers. With respect to electrostatic interaction there exists repulsive forces between the surfaces with same charges and attraction between surfaces with opposite charges.
- Incorporation of zinc in spinel oxide layers stabilizes the spinels, which results in reduction in source term of corrosion products.

## 10 References

- Ahlberg E. and Rebensdorff B., In Proc. BNES Conf. Water Chemistry Nucl. Reactor Syst. 6, Bournemouth, UK, 12-15 Oct. 1992, Vol. 2, 278-5/8, 1992.
- Asakura Y, Uchida S. and Yusa H., Nucl. Sci. Eng. 72, 117-120, 1979
- Asakura, Y., et al., Corrosion NACE, 1989, 45, 119-124.
- ASTM D 3770, *Standard practice for sampling water from closed conduits*, 1999.
- ASTM D 38-64-96, *Standard Guide for Continual On-Line Monitoring Systems for Water Analysis*, Reapproved 2000.
- ASTM D 1066, *Standard practice for sampling steam*, 2001.
- ASTM D 3370-95a, *Standard Practices for Sampling Water from Closed Conduits*, Reapproved 2003.
- BAPL (Bettis Atomic Power Laboratory), *Pressurized water reactor (PWR) project technical progress report for the period January 24, 1964 – April 23, 1964*, WAPD-MRP-108, p. 35, Westinghouse Electric Corporation, Bettis Atomic Power Laboratory, 1964 (Cited in Cohen, 1969).
- Barton M. et al, *Corrosion product measurements at the Sizewell- B PWR International Conference on Water Chemistry in Nuclear Reactor systems*, Bournemouth, 2000.
- Baum A., *Restricted geometries and deposits*, Chapter 6 of the ASME Handbook on Water Technology for Thermal Power Systems. Paul Cohen, Editor-in-Chief, New York: The American Society of Mechanical Engineers, pp. 279-338, 1989.
- Beal S. K., *Deposition of particles in turbulent flow on channel or pipe walls*, Nuclear Science and Engineering, 40 pp. I-II, 1970.
- Bénézech P., Palmer D. A., Wesolowski D. J. and Xiao C., *New measurements of the solubility of zinc oxide from 150 to 350°C*, Journal of Solution Chemistry 31, p. 947-973, 2002.
- Bengtsson B., Aronsson P. -O., Larsson S. and Andersson P. -O., *Experience with elevated pH and Lithium in Ringhals PWRs*, International Conference on Water Chemistry in Nuclear Reactor System, NPC'08, Paper L1-4s, Berlin, Germany, 2008.
- Bengtsson B., *Elevated pH and lithium: Possible tool to reduce radiation source terms*, WANO Workshop on Reduction of Dose Rate in PWRs, Würzburg, 2009.
- Bengtsson B., *Experience concerning corrosion product sampling of reactor coolant*, EPRI RFP-Meeting, Working Group 1 Tampa Florida, Feb. 27-28, 2002.
- Berezina I. D. et al, *Influence of corrosion product transport on fuel assembly reliability of NPP with VVER 440 reactors*, International water conference, Budapest, 2005.
- Berge P., Thesis, Paris University, *Influence des traitements de surface sur la resistance a la corrosion des aciers inoxydables*, 1968.
- Bergmann C. A., Durkosh D. E., Lindsay W. T. and Roesmer J., *The role of coolant chemistry in PWR radiation-field build-up*, EPRI Report NP-4247, 1985.
- Berry W. E. and Diegle R. B., *Survey of Corrosion Product Generation, Transport and Deposition in Light Water Nuclear Reactors*, EPRI Final Report, NP-522, March 1979.

- Beslu P., Jadot F., Noe M., Metge M. and Favennec J., In Proc. BNES Conf. Water Chem. Nucl. Reactor Syst. 4, Paper 20, 57-61, Bournemouth 13-17 Oct., 1986.
- Beverkog B., *AOA Fuel Crud: A Theoretical approach*, International Conference on Water Chemistry of Nuclear Reactor systems, Jeju Island, Korea, Oct. 23-26, 2006.
- Bird E.J., James H. and Symons W.J., In Proc. BNES Conf. Water Chem. Nucl. Reactor Syst. 3 Bournemouth 17-21 Oct. 1983, 153-162, 1983.
- Blok J., Chauffriat S. and Frattini P., *Concentration Factors Required for LiBO<sub>2</sub> Precipitation in AOA*, EPRI AOA Science Workshop, Palo Alto, CA, 10-11 February, 2000.
- Bojinov M., Buddas T., Halin M., Helin M., Kinnunen P., Kvarnström R., Laitinen T., Mutilainen E., Mäkelä K., Reinvald A., Saario T., Sirkiä P. and Tompuri K., In Proceedings of Chimie 2002, International Conference *Water Chemistry in Nuclear Reactor Systems. Operation Optimisation and New Developments*, Avignon, France, SFEN, French Nuclear Energy Society, paper No.143 (CD-ROM publication), 2002.
- Bolz M., Hoffmann W., Rühle W., KKP internal Final Research Reports Part A and B *Aktivitätsaufbau in Leichtwasser Reaktoren; Chemische und radiochemische Untersuchungen; a VGB Research Program*, Curtsey of M. Bolz, 1996b.
- Bolz M., Hoffmann W. and Rühle W., *Characterization of colloids in primary coolant*, International Conference on Water Chemistry of Nuclear Reactor systems 7, BNES, 1996a.
- Bretelle J-L, personal communication, 2013.
- Brüesch P. et al, Anal. Chem. 319, S. 812-821, 1984.
- Byers A. and Deshon J., *CRUD Structure and Chemistry of PWR CRUD*, Proceedings of the International Conference on Water Chemistry of Nuclear Reactor Systems, NPC'08, Paper L13-4, San Francisco, 2004.
- Byers W. A. and Jacko R. J., In Proceedings of the Sixth International Symposium on Environmental Degradation of Materials in Nuclear Power Systems - Water Reactors, The Minerals, Metals and Materials Society, 837-844, 1993.
- Byers W. A., Wang G. and Deshon J. C., *The limits of zinc addition in high duty PWRs*, International Conference on Water Chemistry in Nuclear Reactor Systems, Berlin 2008.
- Camp J. J., *Etude de la corrosion généralisée des Alliages 600 dans le milieu primaire des réacteurs à eau pressurisée, Essais sur la coule BOUCOR*, EDF Report HT/PV D 585 MAT/T42, 1985.
- Caron D., Daret J., Lefevre Y., Santarini G., Mazille H., Benoit R., Erre R., and Cassagne T., In EUROCORR 2000, Institute of Materials, London, 2000.
- Carrette F., Lafont M.C., Chatainier G., Guinard L. and Pieraggi B., Surf. Interf. Anal. 34, 135-138, 2002(cited in [Combrade, 2005]), 2002a.
- Carrette F., Guinard L. and Pieraggi B., In Proceedings of Chimie 2002, International Conference Water Chemistry in Nuclear Reactor Systems. Operation Optimisation and New Developments, Avignon, France, SFEN, French Nuclear Energy Society, 2002b.
- Carrette F., Cattant F., Legras L., Bardet F., Merrer M. and Guinard L., *Impact of the surface state of steam generator tubes on the release of corrosion products in pressurized water reactors*, International Conference on Water Chemistry of Nuclear Reactor Systems, Jeju Island, Korea, October 23-26, 2006.

- Charlesworth D. H., *The deposition of corrosion products in boiling water systems*, Chem. and progr. Symp. Series (AICE Nucl. Eng.), 1970.
- Chauffriat S., Buffiere J. and Frattini P., *Boric Acid Physisorption at the Fuel Deposit Surfaces*, EPRI AOA Science Workshop, Palo Alto, CA, 10-11 February 2000.
- Chen J. and Bengtsson B., *Scanning electron microscopy study on the particulate corrosion products from PWR primary water under different operation and water chemistry conditions*, International Conference on Water Chemistry in Nuclear Reactor systems, Berlin, Germany, 2008.
- Chen J., Bengtsson B., Bergqvist H. and Jädernäs D., *On the phase compositions of fuel crud formed in PWRs using steam generator tubing materials of alloy 600 and 690*, Proceedings of International Conference on Water Chemistry in Nuclear Reactor systems, Paris, France, 2012.
- Chestakov Dr. Ioury, *Probabilistic-Statistical Analysis of VVER Fuel Element Leaking Causes and Comparative Analysis of The Fuel Reliability Indicator on NPP's with VVER and PWR Reactors*, Proc: IAEA Technical meeting on fuel failure in water reactors: causes and mitigation, Bratislava 17-21 June 2002.
- Christensen H. et al., *Radiolysis Modelling and Corrosion Potential Measurements in Nuclear Power Environment*, BNES 3<sup>rd</sup> Workshop on LWR coolant water radiolysis and electrochemistry, Dorset, UK, Oct. 2000.
- Clauzel M. et al, *Correlation between Nickel Base Alloys Surface Conditioning and Cation Release Mitigation in Primary Coolant*, International Conference on Water Chemistry of Nuclear Reactor Systems, Quebec, Canada, 2010.
- Cohen P., *Water Coolant Technology of Power Reactors*, Gordon and Breach Science publishers, New York, London, Paris, 1969.
- Combrade P., Foucault M., Vancon D., Marcus P., Grimal J. -M. and Gelpi A., In Proceedings of the Fourth International Symposium on Environmental Degradation of Materials in Nuclear Power Systems – Water Reactors, NACE International, Houston, 5-79 – 5-94, 1989.
- Combrade P., Scott P.M., Foucault M., Andrieu E., Marcus P., *Oxidation of Ni base alloys in PWR water: Oxide layers and associated damage of the base metal*, 12<sup>th</sup> Inter. Conf. on Deg. of Materials in Nucl. Pow. Syst., 2005.
- Cox B., Garzarolli F., Strasser A. and Rudling, P., *The Effects of Zn Injection (PWRs and BWRs) and Noble Metal Chemistry (BWRs) on Fuel Performance – an Update*, ZIRAT8/IZNA3 Special Topics Report, ANT International, Mölnlycke, Sweden, 2003/2004.
- Dacquait F., Ridoux P., Brun C. and Engler N., *Impact of Steam Generator Replacement on PWR primary circuit contamination by radioactive corrosion products*, Water Chemistry of Nuclear Reactor Systems 8, BNES, p. 53, 2000.
- Dacquait F. et al, *Corrosion Product Transfer in French PWRs during Shutdown*, International Conference on Water Chemistry in Nuclear Reactor Systems, Avignon 2002.
- Da Cunha Belo M., Corros. Sci. 40, 447-463, 1998.
- Darras R., Proceedings Series IAEA-SM-264/37, 1982.
- De Bruyn P. L. D. and Agar G. E., in Fuerstanu D. W., *Froth Floatation, 50<sup>th</sup> Anniversary Volume*, Chapter 5, AIME, New York, 1962.

- Decossin E., Bremnes O. and Tigeras A., *Axial Offset Anomaly Feedback and R&D Modeling Studies on EdF Cores*, Proceedings of the International Conference on Water Chemistry of Nuclear Reactor Systems, Berlin, 2008.
- Degueldre C., Schenker E. and Nobbenhuis-Wedda H., *Water Chemistry of Nuclear Reactor Systems, Vol 1*, BNES, Bournemouth, UK, October, 1996.
- Deshon J., EPRI Report 1003213, *PWR axial offset anomaly (AOA) guidelines*, Rev. 1, 2004.
- Deshon J. and Kucuk A., EPRI- *Fuel Reliability Program, Assessment: Effect of elevated coolant hydrogen on fuel components*, International Workshop on Optimization of Dissolved Hydrogen in PWR Primary Coolant, Tohoku University Sendai, Japan, July 18-19, 2007.
- Dobrevski I., *VVER-1000 Coolant Chemistry Improvement by Extended Fuel Cycles, Optimization of Water Chemistry Technologies and management to Ensure Reliable Fuel Performance at High Burnup and in Ageing Plants (FUWAC)*, IAEA, Turku, Finland, 2009.
- Donaldson A. T. and Vitanza C., *CRUD deposition on Fuel Rods as Consequence of Spikes in the Concentration of Water Additives in a PWR Loop*, OECD HRP, HWR-407, 1994.
- Doncel N., Chen J. and Bergqvist H., *Confirmation of  $\text{Li}_2\text{B}_4\text{O}_7$  Presence in Fuel Crud Formed under Simulated PWR Water Chemistry Conditions*, International Conference on Water Chemistry of Nuclear Reactor systems, Jeju Island, Korea, Oct. 23-26, 2006, 2006a.
- Doncel N., Rubio G., Novo M., Mata P., Remartinez B., Deshon J. and Chen J., *Experimental verification of water chemistry influence on AOA*, Top-Fuel-Salamanca, 2006b.
- Doncel N. and Chen J., *Water Chemistry Influence on AOA – Phase 3 of the Spanish Experiment at Studsvik*, Proceedings of the 2007 International LWR Fuel Performance Meeting, San Francisco, CA, Sept. 30 - Oct 3, 2007.
- Doncel N. et al., *On the Role of Nickel Deposition in a CIPS Occurrence in PWR*, International Conference on Water Chemistry of Nuclear Reactor Systems, Berlin, Germany, 2008.
- Dudjakova K., Kysela J., Zmitko M., Martykan M., Janesik J. and Hanus V., 6<sup>th</sup> International Seminar on Primary and Secondary Side Water Chemistry of NPP, Budapest, 2005.
- Eater L., *Make sure water chemistry samples are representative*, Power, July 1989.
- Engler N., Brun C., and Guillodo N., *Optimization of SG-Tubes Prefilming Process to Reduce Nickel Release*, International Conference on Water Chemistry of Nuclear Reactor Systems, Berlin, 2008.
- EPRI Report NP-2968, *Primary-Side Deposits on PWR Steam Generator Tubes*, 1983.
- EPRI, *BWR Coolant Impurity Identification Study*, EPRI Report NP-4156, August, 1985.
- EPRI Report NP-6640, *The Nature of Behavior of Particulates in PWR Primary Coolant*, December 1989.
- EPRI Report TR-108320, *Root cause investigation of axial offset anomalies*, June 1997a.
- EPRI Report TR-108783, *Impact of PWR Chemistry on Corrosion product deposition on Fuel cladding Surfaces*, November 1997b.
- EPRI Report 1003212, *Experimental Verification of the Root Cause Mechanism for Axial Offset Anomaly*, December 2002.
- EPRI PWR Primary Water Chemistry Guidelines: Revision 5, TR1002884, September 2003.